

Fronthaul-Aware User-Centric Generalized Cell-Free Massive MIMO Systems

Zahra Mobini, *Member, IEEE*, Ahmet Hasim Gokceoglu, Li Wang, *Member, IEEE*, Gunnar Peters
and Hien Quoc Ngo, *Fellow, IEEE*

Abstract—We consider fronthaul-limited generalized zero-forcing-based cell-free massive multiple-input multiple-output (CF-mMIMO) systems with multiple-antenna users and multiple-antenna access points (APs) relying on both cooperative beamforming (CB) and user-centric (UC) clustering. The proposed framework is very general and can be degenerated into different special cases, such as pure CB/pure UC clustering, or fully centralized CB/fully distributed beamforming. We comprehensively analyze the spectral efficiency (SE) performance of the system wherein the users use the minimum mean-squared error-based successive interference cancellation (MMSE-SIC) scheme to detect the desired signals. Specifically, we formulate an optimization problem for the user association and power control for maximizing the sum SE. The formulated problem is under per-AP transmit power and fronthaul constraints, and is based on only long-term channel state information (CSI). The challenging formulated problem is transformed into tractable form and a novel algorithm is proposed to solve it using minorization maximization (MM) technique. We analyze the trade-offs provided by the CF-mMIMO system with different number of CB clusters, hence highlighting the importance of the appropriate choice of CB design for different system setups. Numerical results show that for the centralized CB, the proposed power optimization provides nearly 59% improvement in the average sum SE over the heuristic approach, and 312% improvement, when the distributed beamforming is employed.

Index Terms—Cell-free massive multiple-input multiple output (CF-mMIMO), cooperative beamforming, fronthaul, resource allocation, sum spectral efficiency (SE).

I. INTRODUCTION

Cell-free massive multiple-input multiple-output (CF-mMIMO) is a promising wireless networking platform that can effectively cater to the pervasive connectivity needs and escalating demands for data traffic in the realm of beyond fifth generation (5G). The key idea of CF-mMIMO is to deploy many geographically distributed access points (APs) in the coverage area without dividing the area into disjoint cells. The APs coordinate through multiple central processing units (CPUs) and coherently serve multiple users in the same time-frequency resources [1], [2]. However, in practical implementations, the gains of CF-mMIMO systems might saturate with the number of users and coordinating APs due to the significant overhead required to acquire data, knowledge

of the channel state information (CSI), and beamforming matrix over the fronthaul network and also due to the channel estimation errors. Moreover, serving users by far APs may not be reasonable due to the fact that they consume valuable radio resources but provide users with low improvement in the signal power.

As a remedy, the concept of dynamic cooperation clusters has been integrated into CF-mMIMO systems, gaining significant attention in recent years, particularly with the emergence of user-centric (UC) CF mMIMO [3], [4]. In UC CF-mMIMO a small set of distributed (single or few antenna) APs jointly serve a subset of users with assumption of high density of antennas with respect to the number of users. UC CF-mMIMO exhibits a remarkable capability for maximizing the efficient utilization of limited power and bandwidth resources, delivering performance that is close to that of the canonical cell-free network in terms of achievable data rate. Moreover, it demands reduced fronthaul/backhaul bandwidth and complexity, rendering it scalable for practical implementations [4]. The benefits of dynamic resource allocation and user scheduling for the UC CF-mMIMO networks were investigated in [5] where the total downlink achievable rate is maximized under the user's rate requirement. The two-stage proposed framework in [5] first partitions users into groups and then groups are scheduled on different frequencies. The corresponding optimization problems were solved by using semi-definite relaxation (SDR) and sequential convex approximation (SCA)-based approach, respectively. In [6] user scheduling, power allocation, and beamforming were optimized for UC CF-mMIMO networks given the limited number of users to maximize sum rate for both the coherent and non-coherent transmission modes. The authors in [6] resorted to tools from fractional programming, block coordinate descent, and compressive sensing to construct the beamforming weights and user scheduling algorithms. Total energy efficiency of UC CF-mMIMO with AP selection and power control was investigated in [7], [8] where it was shown that power allocation algorithm together with the AP selection can notably enhance the energy efficiency. In [7] power control with received-power-based AP selection and channel-quality-based AP selection were studied to decrease the power consumption caused by the fronthaul links. The proposed algorithms in [7] rely on heuristics to specify AP selections. The authors in [8] jointly optimized the downlink power control and the active APs (considering ON/OFF activity for the APs) to minimize the total transceiver power consumption under the per-user minimum downlink ergodic spectral efficiency (SE)

Z. Mobini and H. Q. Ngo are with the Centre for Wireless Innovation (CWI), Queen's University Belfast, BT3 9DT Belfast, U.K. (email: {zahra.mobini, hien.ngo}@qub.ac.uk). H. Q. Ngo is also with the Department of Electronic Engineering, Kyung Hee University, Yongin-si, Gyeonggi-do 17104, Republic of Korea. A. gokceoglu1, L. Wang, and G. Peters are with the Huawei's Sweden Research Center, Stockholm, Sweden (e-mail: {ahmet.hasim.gokceoglu1, leo.li.wang, gunnar.peters}@huawei.com). (Corresponding authors: Hien Quoc Ngo.)

constraint. Joint user association and power allocation schemes were proposed in [9] for cell-free visible light communication (VLC) networks to address load balancing and power control issues. Meanwhile, different optimization schemes tailored to the varying sizes of CF-mMIMO systems were introduced in [10]. Learning-based approaches were also employed as an alternative to model-based optimization methods for designing optimal power control [11], user association schemes [12], and precoding design [13].

The ongoing research efforts on CF-mMIMO systems have mainly focused on non-coordinating beamforming strategies such as matched filtering (MF) [1], local zero forcing (ZF) [10], [14], and the combination of centralized ZF with maximum-ratio transmission (MRT) [15] to reduce the fronthaul overhead and complexity. However, the performance of CF-mMIMO systems can be considerably improved by using cooperative beamforming (CB) among the APs. There are two ways to implement CB 1) centralized beamforming, and 2) distributed beamforming. In the centralized beamforming schemes all the APs send local channel estimates to the CPU through fronthaul links. The CPU computes beamforming matrix, and then sends the optimized beamforming to the APs. This requires huge CSI exchange between the APs and the CPU and more importantly high massive computational complexity for the large number of APs/users regime. Nevertheless, modern CPUs equipped with many processors and hence distributed algorithms for beamforming could be designed to leverage these multi-core processors. CF-mMIMO with centralized coordinated ZF-based beamforming designs has been studied in [16], [17], while centralized minimum mean-squared error-based (MMSE) design has been investigated in [18] with different levels of coordination. In contrast, deep learning-based coordinated beamforming design has been proposed in [13] for traditional cellular systems, focusing on multicell downlink scenarios with rate-limited CSI exchange between base stations (BSs).

It is imperative to note that research on CF-mMIMO with CB and/or UC clustering is still in its infancy, with numerous key challenges yet to be addressed [19], such as following: *i)* From a performance perspective, fully centralized CB is optimal but impractical for many real-world scenarios due to its scalability issues, requiring extensive cooperation and a costly fronthaul/backhaul network. Conversely, fully distributed (non-coordinating) beamforming, where the beamforming design is handled locally at the APs, is scalable, and has low implementation demands but yields mediocre performance. Therefore, studying the trade-offs between the performance, scalability, and degree of cooperation among the APs in general CF-mMIMO systems with UC clustering for different application scenarios is meaningful and important. *ii)* Furthermore, most studies tend to investigate simple system setup where the users are equipped with single antenna. However, in practice, users can be equipped with multiple antennas to improve system reliability due to the higher diversity gain [20]. The extension of the CF-mMIMO to the case with multiple-antenna users is not trivial, especially for the CF-mMIMO with no downlink channel estimation in

which channel-dependent combining schemes cannot be used at the user sides. *iii)* In addition, most of the above mentioned studies consider the case in which the APs are managed by one or several CPUs to which they are connected through an infinite fronthaul/backhaul capacity links. However, the assumption of infinite fronthaul is not realistic in practice. In fact, the limited fronthaul capacity constitute one of the most key challenges in practical CF-mMIMO systems. The performance of a CF-mMIMO system with single-antenna users and non-coordinating beamforming design in the uplink and downlink, taking account the fronthaul constraint, has been investigated in [21], [22], and [23], respectively. Coordinated beamforming design for a reconfigurable intelligent surface (RIS)-aided CF-mMIMO system with single-antenna users under CSI uncertainties at the transmitter and the capacity-limited fronthaul links was investigated in [24]. Moreover, distributed resource allocation algorithms for user scheduling and beamforming in a UC CF-mMIMO system were studied in [25]. However, the authors in [25] assumed single-antenna users and infinite fronthaul capacity links. Additionally, resource allocation in [25] relied on instantaneous CSI rather than statistical CSI. Therefore, all designs must be quickly re-computed whenever the small-scale fading coefficients change. Moreover, they necessitate instantaneous CSI knowledge at the users, leading to significant overhead in systems with many users. We would like to highlight that [20] pursued a performance analysis of CF-mMIMO systems with multi-antenna users, while the CB and UC designs were ignored, and the impact of limited fronthaul capacity links was not investigated either. To the best of the authors' knowledge, the performance of fronthaul-limited CF-mMIMO, which relies on both UC and CB alongside multiple-antenna users, has not been studied. Motivated by filling the above-mentioned knowledge gaps in the literature, we consider a fronthaul-limited UC generalized CF-mMIMO systems with multiple antennas at both APs and users, where the available APs are divided into multiple disjoint CB clusters. APs in each CB cluster perform ZF-based CB and send data symbols to a subset (not all) of the users in the system. Then, the SE of the system is investigated comprehensively.

The key contributions of this paper are summarized as follows:

- We provide an analytical framework for a fronthaul limited CF-mMIMO system with multiple-antenna users/APs and the notion of joint CB and UC clustering wherein the users use the minimum mean-squared error-based successive interference cancellation (MMSE-SIC) scheme to detect the desired signals. The proposed CF-mMIMO framework is very general and can cover different CF-mMIMO scenarios. In particular, it can be degenerated to different special cases such as conventional CF-mMIMO with pure CB, pure UC clustering, fully centralized beamforming, and fully distributed beamforming.
- We formulate a novel optimization problem for the user association and power control of the generalized CF-mMIMO system for maximizing the sum SE. The formulated problem is under per-AP transmit power and

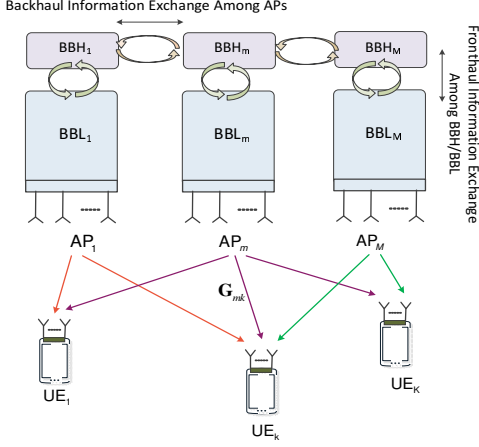


Fig. 1: Illustration of a CF-mMIMO with BBH and BBL architecture.

fronthaul constraints. We solve the sum-SE maximization problem by casting the original problem into two sub-problems, namely P1) power optimization given user-association and P2) user association given power optimization.

- We show that the power optimization in P1 is non-convex and thus we propose a novel algorithm to solve the challenging formulated problem. In particular, we resort to sequential optimization framework, also known as minorization maximization (MM) approach. By using this iterative framework, we reformulate the original non-convex power optimization problem into a series of auxiliary convex subproblems that can be easily solved by algorithms that have low computational complexity and their solutions converge to a locally optimal solution of the original problem. Following P1, we propose a scheme based on channel gain criterion to address the user association problem in P2.
- Numerical results confirm that our joint optimization approach significantly outperforms the heuristic approaches. The simulation results also show the different trade-offs between the performance and degree of cooperation among the APs in general CF-mMIMO systems. More precisely, the proposed power allocation scheme yields increasing benefits as the size of CB clusters (number of coordinating APs) decreases, i.e., when interference cancellation via beamforming is limited. Furthermore, as the beamforming capability of APs improves (with more antennas per AP), the proposed power allocation significantly enhances fully distributed beamforming performance, reducing the need for beamforming coordination among APs. In addition, our results indicate that under practical fronthaul limitations, the proposed power allocation combined with simple distributed CB architecture can even outperform a computationally-heavy fully centralized CB without power control.

Notation: We use bold upper case letters to denote matrices, and lower case letters to denote vectors. The superscript $(\cdot)^H$ stands for the conjugate-transpose and $\text{tr}(\cdot)$ shows the transpose. A zero-mean circular symmetric complex Gaussian

distribution having a variance of σ^2 is denoted by $\mathcal{CN}(0, \sigma^2)$, while \mathbf{I}_N denotes the $N \times N$ identity matrix. Finally, $\mathbb{E}\{\cdot\}$ denotes the statistical expectation.

II. SYSTEM MODEL AND BEAMFORMING DESIGN

We consider a CF-mMIMO system that consists of M APs and K users. Each AP and user are equipped with L antennas and N antennas, respectively. We also consider functional split for baseband unit (BBU). More specifically, computational functions at BBUs are split into two entities called baseband low (BBL) and baseband high (BBH), as shown in Fig. 1. The BBH is responsible for managing processing tasks such as beamforming, encoding, and radio resource management, while the BBL is responsible for processing tasks such as weight applications, error correction, and modulation. BBHs are connected through limited-capacity fronthaul links¹ to their associated BBLs for sending information such as beamforming matrices/vectors, data, and power coefficients. Moreover, BBHs are connected through backhaul links for information exchange between APs.

We assume a frequency-flat slow fading channel model for each orthogonal frequency-division multiplexing (OFDM) subcarrier. In the sequel, the subcarrier index will be omitted for the sake of notational simplicity. Let $\mathbf{G}_{mk} \in \mathbb{C}^{L \times N}$ be the complex channel matrix between the m -th AP, and the k -th user. It can be modeled as

$$\mathbf{G}_{mk} = \beta_{mk}^{1/2} \mathbf{H}_{mk}, \quad (1)$$

where β_{mk} denotes the large-scale fading coefficient that includes path-loss and shadowing effects, while $\mathbf{H}_{mk} \in \mathbb{C}^{L \times N}$ is the small-scale fading matrix whose entries are i.i.d. $\mathcal{CN}(0, 1)$ random variables. Large-scale fading coefficients change slowly and may be constant in range of many small-scale fading coherence intervals (over time and frequency bands). Hence, it is assumed that these coefficients are priori known at each BBL/BBH.

The system is operating according to a time division duplex (TDD) protocol, i.e., the uplink and downlink transmissions occur at different times but use the same frequency. Here, we focus on the downlink and hence, consider two-phase transmission protocol wherein each coherence interval divides into uplink training phase and downlink data transmission phase. By exploiting uplink/downlink channel reciprocity, the downlink CSI can be estimated through uplink training. Let us denote the length of the TDD interval by τ_c , which is determined by the shortest coherence interval of all users in the network. Also, denote τ_u as the length of the uplink training phase per coherence interval.

We consider CF-mMIMO with the notion of joint CB and UC clustering. We note that in the sequel, the set of APs that send signal to user k is called UC cluster of user k and the set of coordinated APs that exchange CSI and perform CB is called CB cluster. In the downlink data transmission phase, APs perform CB and send data symbols to a subset of the users in the system. In particular, for CB clustering

¹In some literature, the term “backhaul” denotes the link between BBL and BBH when adopting a functional split in BBU. In this paper, we interchangeably use “fronthaul” to denote the same link, without loss of generality.

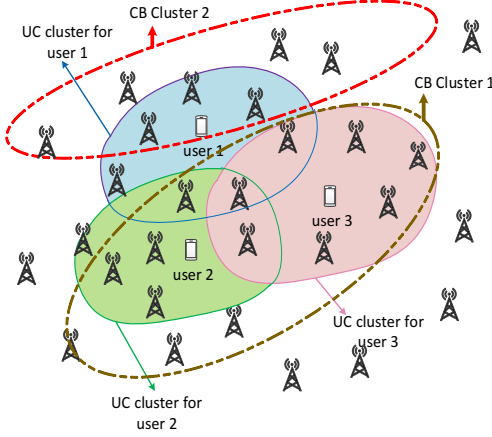


Fig. 2: CF-mMIMO with UC and CB clustering approaches.

the available APs are divided into C disjoint CB clusters. APs in each CB cluster share CSIs such that they have CSI knowledge of all the users assigned to the APs in this cluster and perform coordinated beamforming. Figure 2 illustrates an example of CF-mMIMO that includes three users served by a large number of APs, three UC clusters and two CB clusters. The coloured regions show which UC clusters of AP are serving which users. Clearly, the UC clusters are partially overlapping which results from the core feature of the cell-free networks. Moreover, the red and brown regions show the clusters for CSI exchange and CB.

It is noteworthy that the proposed framework for CF-mMIMO with CB and UC clustering is very general and can be degenerated to four special cases as conventional CF-mMIMO with pure CB, CF-mMIMO with pure UC clustering, UC CF-mMIMO with fully centralized beamforming and UC CF-mMIMO with fully distributed beamforming as will be discussed in further details in the next sections. In the following we will summarize the uplink training and downlink payload transmission phases in more details.

A. Uplink Training

During the uplink training phase, all users send pilot signals to the APs. Accordingly, each AP can estimate the corresponding channels to all the users using the obtained pilot signal. Note that at each AP, the channel estimation is performed at its BBH. Let us denote by $\Phi_{u,k} \in \mathbb{C}^{\tau_u \times N}$ the pilot matrix of the k -th user where its n -th column satisfies $\|\phi_{u,k,n}\|^2 = 1$, $\forall n \in N$. The received signal at the m -th AP can be written as

$$\mathbf{Y}_{u,m} = \sum_{k=1}^K \sqrt{\tau_u} P_u \mathbf{G}_{mk} \Phi_{u,k}^H + \mathbf{W}_{u,m}, \quad (2)$$

where P_u is the transmit power of each uplink pilot symbol and $\mathbf{W}_{u,m} \in \mathbb{C}^{L \times \tau_u}$ is the complex additive Gaussian noise matrix at the m -th AP whose elements are i.i.d. $\mathcal{CN}(0, \sigma^2)$. By projecting $\mathbf{Y}_{u,m}$ onto $\Phi_{u,k}$, we get

$$\begin{aligned} \mathbf{Y}_{u,mk} &= \mathbf{Y}_{u,m} \Phi_{u,k} \\ &= \sum_{i=1}^K \sqrt{\tau_u} P_u \mathbf{G}_{mi} \Phi_{u,ik} + \mathbf{W}_{u,mk}, \end{aligned} \quad (3)$$

where $\Phi_{u,ik} = \Phi_{u,i}^H \Phi_{u,k}$ and $\mathbf{W}_{u,mk} = \mathbf{W}_{u,m} \Phi_{u,k}$. Now, the estimate of the channel matrix \mathbf{G}_{mk} can be calculated as [20]

$$\hat{\mathbf{G}}_{mk} = \mathbf{Y}_{u,mk} \mathbf{A}_{mk}, \quad (4)$$

where

$$\mathbf{A}_{mk} \triangleq \sqrt{\tau_u P_u \beta_{mk}} \left(\tau_u P_u \sum_{i=1}^K \beta_{mi} \Phi_{u,ik}^H \Phi_{u,ik} + \sigma^2 \mathbf{I}_N \right)^{-1}. \quad (5)$$

Remark 1. In the case that pilot sequences assigned to the users are pairwise orthonormal, we have $\Phi_{u,ik} = \mathbf{I}_N$, when $i = k$. Otherwise $\Phi_{u,ik} = \mathbf{0}$. Then (5) becomes

$$\mathbf{A}_{mk} = c_{mk} \mathbf{I}_N. \quad (6)$$

where $c_{mk} \triangleq \frac{\sqrt{\tau_u P_u \beta_{mk}}}{\tau_u P_u \beta_{mk} + \sigma^2}$. Moreover, (3) simplifies to

$$\mathbf{Y}_{u,mk} = \sqrt{\tau_u P_u} \mathbf{G}_{mk} + \mathbf{W}_{u,mk}, \quad (7)$$

and accordingly thermal noise is the only disturbance harming the channel estimate. A necessary condition for this to happen is $\tau_u \geq KN$. The estimation error is given by $\tilde{\mathbf{G}}_{mk} = \mathbf{G}_{mk} - \hat{\mathbf{G}}_{mk}$ with $\tilde{\mathbf{G}}_{mk}$ and $\hat{\mathbf{G}}_{mk}$ are independent and have i.i.d. $\mathcal{CN}(0, \gamma_{mk})$ and i.i.d. $\mathcal{CN}(0, \beta_{mk} - \gamma_{mk})$ elements, respectively, where γ_{mk} is the mean-square of the estimate, i.e., for any element $[\hat{\mathbf{G}}_{mk}]_{ij}$ we have $\gamma_{mk} \triangleq \frac{\tau_u P_u \beta_{mk}^2}{\tau_u P_u \beta_{mk} + \sigma^2}$.

B. Downlink Data Transmission and Beamforming Design

In CF-mMIMO with UC clustering, each AP communicates only with a subset of users in the network. The procedure for the selection of the users to serve, i.e., determining the UC clusters, will be specified in the next section. Denote by \mathcal{K}_m the set of users served by the m -th AP and define $K_m = |\mathcal{K}_m|$ as the number of users in \mathcal{K}_m . Now, for all the subsets \mathcal{K}_m , $m = 1, \dots, M$, we can define the set \mathcal{M}_k as the set of all APs that serve the k -th user, i.e.,

$$\mathcal{M}_k = \{m : k \in \mathcal{K}_m\},$$

with $M_k = |\mathcal{M}_k|$. Let \tilde{N} be the number of independent downlink data streams sent to each user, $\tilde{N} \leq N$. To be more general and to reduce the amount of data traffic to be fronthauled between BBHs and BBLs, we suppose \tilde{N} can take an integer value from 1 to N . We assume that \mathbf{x}_k is the vector of \tilde{N} symbols, intended for the k -th user, $\mathbb{E}\{\mathbf{x}_k \mathbf{x}_k^H\} = \mathbf{I}_{\tilde{N}}$. Accordingly, the $L \times 1$ signal transmitted by the m -th BBL can be expressed as

$$\mathbf{s}_m = \sqrt{P} \sum_{k \in \mathcal{K}_m} \eta_{mk}^{1/2} \mathbf{Q}_{mk} \mathbf{x}_k, \quad (8)$$

where \mathbf{Q}_{mk} denotes the downlink beamforming matrix associated with the k -th user. Moreover, P denotes the AP transmit power and η_{mk} represents the k -th user power control coefficient which needs to satisfy the power constraint at each AP, i.e., $\mathbb{E}\{\|\mathbf{s}_m\|^2\} \leq P$. The k -th user receives signal contributions from all the APs; the observable vector is given by

$$\begin{aligned} \mathbf{r}_k &= \sum_{m=1}^M \mathbf{G}_{mk}^H \mathbf{s}_m + \mathbf{n}_k \\ &= \sqrt{P} \sum_{m \in \mathcal{M}_k} \sum_{k' \in \mathcal{K}_m} \eta_{mk'}^{1/2} \mathbf{G}_{mk'}^H \mathbf{Q}_{mk'} \mathbf{x}_{k'} + \mathbf{n}_k, \end{aligned} \quad (9)$$

where $\mathbf{n}_k \in \mathbb{C}^{N \times 1}$ is the noise vector whose elements are i.i.d. $\mathcal{CN}(0, \sigma^2)$. We can equivalently reformulated (9) as

$$\mathbf{r}_k = \sqrt{P} \sum_{m \in \mathcal{M}_k} \eta_{mk}^{1/2} \mathbf{G}_{mk}^H \mathbf{Q}_{mk} \mathbf{x}_k + \sqrt{P} \sum_{\substack{k'=1 \\ k' \neq k}}^K \sum_{m \in \mathcal{M}_{k'}} \eta_{mk'}^{1/2} \mathbf{G}_{mk'}^H \mathbf{Q}_{mk'} \mathbf{x}_{k'} + \mathbf{n}_k. \quad (10)$$

The first term is the desired signal, the second term describes the multi-user interference (all the signal components intended for user $k', k' \neq k$).

In order to mitigate interference from other APs, we employ ZF-based CB which enables a cluster of APs to share their local CSI and construct ZF precoder to cancel the intra-cluster interference. Let \mathcal{C}_m denotes the set of APs which are in the same CB cluster with AP m and define $C_m = |\mathcal{C}_m|$ as the number of APs in \mathcal{C}_m . Specifically, if AP n and AP m belong to the same CB cluster then $\mathcal{C}_n = \mathcal{C}_m$. Let us denote the set \mathcal{U}_m by the union of the sets $\mathcal{K}_{m'}$ for $m' \in \mathcal{C}_m$, as

$$\mathcal{U}_m = \bigcup_{m' \in \mathcal{C}_m} \mathcal{K}_{m'}.$$

Clearly, each user in \mathcal{U}_m is served by at least one of the APs in \mathcal{C}_m . Since UC clusters are partially overlapping, there might be repeated user indices in \mathcal{U}_m . In this case, repeated indices are removed and \mathcal{U}_m is updated to include only the unique entries of the user indices.

Let $\hat{\mathbf{G}}_m$ be an $(LC_m) \times (NU_m)$ collective channel estimation matrix for corresponding APs in set \mathcal{C}_m , where $U_m = |\mathcal{U}_m|$ denotes the number of users in \mathcal{U}_m . More specifically, $\hat{\mathbf{G}}_m$ consists of $C_m U_m$ blocks of dimension $L \times N$, $\hat{\mathbf{G}}_{ij}$, each corresponding to a particular AP i in set \mathcal{C}_m and user j in set \mathcal{U}_m as

$$\hat{\mathbf{G}}_m = [\hat{\mathbf{G}}_{ij} : i \in \mathcal{C}_m, j \in \mathcal{U}_m]. \quad (11)$$

Now, by employing ZF precoding technique the whole CB matrix constructed for the APs in \mathcal{C}_m , $\bar{\mathbf{Q}}_m \in \mathbb{C}^{(LC_m) \times (NU_m)}$, can be written as

$$\bar{\mathbf{Q}}_m = \hat{\mathbf{G}}_m \left(\hat{\mathbf{G}}_m^H \hat{\mathbf{G}}_m \right)^{-1}. \quad (12)$$

The CB matrix for APs in set \mathcal{C}_m can be rewritten as $\bar{\mathbf{Q}}_m^{\text{ZF}} = \bar{\mathbf{Q}}_m \bar{\mathbf{P}}$, where $\bar{\mathbf{P}}$ includes the power allocation coefficients. To avoid interference toward the users in \mathcal{U}_m , $\hat{\mathbf{G}}_m^H \bar{\mathbf{Q}}_m^{\text{ZF}}$ should be diagonal [16] and hence it is necessary to have $\eta_{m'k} = \eta_{k, \mathcal{C}_m}$, $\forall m' \in \mathcal{C}_m$. That is, in a given CB cluster, power coefficients are only functions of k and η_{k, \mathcal{C}_m} shows the power coefficient allocated for all APs in set \mathcal{C}_m to user k . Thus, the beamforming matrix can be further expressed as

$$\bar{\mathbf{Q}}_m^{\text{ZF}} = \bar{\mathbf{Q}}_m \mathbf{P}_m, \quad (13)$$

where \mathbf{P}_m is an $NU_m \times NU_m$ block diagonal matrix with the j -th matrix on the diagonal $\eta_{k, \mathcal{C}_m}^{1/2} \mathbf{I}_N$ and j is the index of user k in set \mathcal{U}_m . Here, we also note that to implement ZF-based precoding, the total number of transmit antennas at APs in CB \mathcal{C}_m , must meet the requirement $LC_m \geq NU_m$.

Since $\bar{N} \leq N$, we employ singular value decomposition (SVD) technique which enables each BBH to construct its precoding matrix from the whole beamforming matrix designed for each CB cluster. Performing the SVD of $\hat{\mathbf{G}}_m$ yields

$$\hat{\mathbf{G}}_m = \mathbf{U}_m \Sigma_m \mathbf{V}_m^H, \quad (14)$$

where the matrices $\mathbf{U}_m \in \mathbb{C}^{(LC_m) \times (NU_m)}$ and $\mathbf{V}_m \in$

$\mathbb{C}^{(NU_m) \times (NU_m)}$ contain, the left and right singular vectors and Σ_m includes singular values in nonascending order, corresponding to the non-zero eigenmodes, respectively. Substituting (14) into (12), we have

$$\begin{aligned} \bar{\mathbf{Q}}_m &= \mathbf{U}_m \Sigma_m \mathbf{V}_m^H (\mathbf{V}_m \Sigma_m \mathbf{U}_m^H \mathbf{U}_m \Sigma_m \mathbf{V}_m^H)^{-1} \\ &= \mathbf{U}_m \Sigma_m \mathbf{V}_m^H (\mathbf{V}_m \Sigma_m^2 \mathbf{V}_m^H)^{-1} \\ &= \mathbf{U}_m \Sigma_m^{-1} \mathbf{V}_m^H. \end{aligned} \quad (15)$$

Now, each BBH can construct its precoding matrix for transmission to user k by choosing the corresponding \bar{N} column vectors associated to its strongest singular values as expressed in (16). In particular, let AP m correspond to the i -th element of set \mathcal{C}_m , $i \in \{1, \dots, C_m\}$, and user k correspond to the j -th element of set \mathcal{U}_m , $j \in \{1, \dots, U_m\}$, then we set $\omega_{mk} = i$ and $\nu_{mk} = j$, respectively. Accordingly, the downlink beamforming matrix constructed for the m -th AP to the k -th user can be calculated as the submatrix of $\bar{\mathbf{Q}}_m$ obtained by selecting the L rows a_{mk} to \check{a}_{mk} and \bar{N} columns b_{mk} to \check{b}_{mk} as

$$\begin{aligned} \mathbf{Q}_{mk} &= [\bar{\mathbf{Q}}_m]_{(a_{mk}:\check{a}_{mk}, b_{mk}:\check{b}_{mk})} \\ &= \mathbf{U}_{mk} \Sigma_m^{-1} \mathbf{V}_{mk}^H, \end{aligned} \quad (16)$$

where $\mathbf{U}_{mk} \triangleq [\mathbf{U}_m]_{(a_{mk}:\check{a}_{mk}, :)}$ with $a_{mk} = (\omega_{mk} - 1) \times L + 1$ and $\check{a}_{mk} = a_{mk} + L - 1$. Also, $\mathbf{V}_{mk}^H \triangleq [\mathbf{V}_m^H]_{(:, b_{mk}:\check{b}_{mk})}$ with $b_{mk} = (\nu_{mk} - 1) \times N + 1$ and $\check{b}_{mk} = b_{mk} + \bar{N} - 1$.

We note that, in the proposed low complexity ZF-based CB all the channels \mathbf{G}_{ij} between AP i , $i \in \mathcal{C}_m$, and user j , $j \in \mathcal{U}_m$, are accounted in CB design of cluster \mathcal{C}_m . However, according to the UC clustering, each AP i may not transmit to one or some of the users in \mathcal{U}_m or equivalently each user j may not be served by one or some of the APs in \mathcal{C}_m . This might affect the orthogonality in beamforming design and result intra-cluster interference. We argue that, in real life CF-mMIMO scenario with efficient UC clustering, the portion of this intra-cluster interference is insignificant compared to the desired signal. The main reason is that those APs that are far from a given user j and have smaller channel gains are not selected for UC cluster of user j , which can be interpreted as the non-orthogonality and intra-cluster interference due to the proposed CB design is negligible and does not degrade the performance. We will justify this assumption in Section V.

III. PERFORMANCE ANALYSIS AND FRONTHAUL REQUIREMENTS

In this section, we first present analytical expression for the SE of the CF-mMIMO with CB assuming that each user uses MMSE-SIC scheme to detect the desired symbols. Moreover, we provide a practical formulation for the fronthaul requirement of CF-mMIMO with BBH-BBL operation.

A. Performance Analysis

The received signal at the k -th user can be rewritten as

$$\mathbf{r}_k = \sqrt{P} \sum_{k'=1}^K \mathbf{D}_{kk'} \mathbf{x}_{k'} + \mathbf{n}_k, \quad (17)$$

where $\mathbf{D}_{kk'} = \sum_{m \in \mathcal{M}_{k'}} \eta_{k', \mathcal{C}_m}^{1/2} \mathbf{G}_{mk'}^H \mathbf{Q}_{mk'}$. Accordingly, we can derive an achievable downlink SE of user k as follows.

Proposition 1. For general CF-mMIMO with ZF-based CB given statistic CSI² and using MMSE-SIC detectors, an achievable downlink SE of user k can be calculated as

$$R_k = (1 - \tau_u / \tau_c) \log_2 \left| \mathbf{I}_{\bar{N}} + P \bar{\mathbf{D}}_{kk}^H \left(\Psi_{kk}^b \right)^{-1} \bar{\mathbf{D}}_{kk} \right|, \quad (18)$$

where

$$\bar{\mathbf{D}}_{kk} = \sum_{m \in \mathcal{M}_k} \eta_{k, \mathcal{C}_m}^{1/2} \mathbb{E} \{ \mathbf{G}_{mk}^H \mathbf{Q}_{mk} \}, \quad (19)$$

and

$$\Psi_{kk}^b = P \mathbb{E} \left\{ \sum_{k'=1}^K \mathbf{D}_{kk'} \mathbf{D}_{kk'}^H \right\} - P \bar{\mathbf{D}}_{kk} \bar{\mathbf{D}}_{kk}^H + \sigma^2 \mathbf{I}_N.$$

Proof. The achievable downlink SE of the k -th user, $k \in \mathcal{K}_m$, with MMSE-SIC detection scheme for the received signal \mathbf{r}_k in (17) and side information Θ_k (assuming that Θ_k is independent of \mathbf{x}_k) is given by [20]

$$R_k = (1 - \tau_{\text{tot}} / \tau_c) \mathbb{E} \{ \log_2 |\mathbf{I}_{\bar{N}} + \Upsilon_{kk}^a| \}, \quad (20)$$

where

$$\Upsilon_{kk}^a \triangleq P \mathbb{E} \{ \mathbf{D}_{kk}^H | \Theta_k \} (\Psi_{kk}^a)^{-1} \mathbb{E} \{ \mathbf{D}_{kk} | \Theta_k \}, \quad (21)$$

and

$$\begin{aligned} \Psi_{kk}^a &\triangleq \mathbf{I}_N + \mathbb{E} \left\{ \left(P \sum_{k'=1}^K \mathbf{D}_{kk'} \mathbf{D}_{kk'}^H | \Theta_k \right) \right\} - P \mathbb{E} \{ \mathbf{D}_{kk} | \Theta_k \} \\ &\quad \times \mathbb{E} \{ \mathbf{D}_{kk}^H | \Theta_k \}. \end{aligned} \quad (22)$$

with τ_{tot} denotes the total training duration for each coherence interval. Given statistic CSI, we have $\Theta_k = \bar{\mathbf{D}}_{kk} = \mathbb{E} \{ \mathbf{D}_{kk} \}$ and $\tau_{\text{tot}} = \tau_u$ and hence, using (20), we can obtain (18). \square

Note that to obtain (18), user k needs to know only the statistical properties of the channels. Therefore, there is no need for downlink pilots, which can reduce the resources required for downlink channel estimation, such as transmit power and estimation overhead. This achievable SE corresponds the rate obtained from the hardening bounding technique which is widely used in massive MIMO literature.

Remark 2. The SE analysis in Proposition 1 is general and holds for different UC and CB clustering schemes. When each user is served by a set of APs, $M_k \leq M$ and $C_m = 1, \forall m$, we have CF-mMIMO with pure UC approach. In contrast, when each user served by all the APs, i.e., $M_k = M, \forall k$, and $C_m > 1$, we have CF-mMIMO with pure CB approach. Further, the SE expression for CF-mMIMO can be easily computed for any \mathcal{C}_m and the corresponding \mathcal{U}_m set. Two important special cases of CB clustering are described below and compared with each other in Section V by means of numerical results.

1) *CF-mMIMO with Fully Centralized Beamforming:* In the case of CF-mMIMO with fully centralized beamforming which is a form of network MIMO all the CSIs are exchanged by all the APs (through the backhaul links between BBHs) to cancel interference. More specifically, there is one CB cluster consists of all APs in the network or equivalently $\mathcal{C}_m = \{1, \dots, M\}, \forall m$, $\mathcal{U}_m = \mathcal{U} = \{1, \dots, K\}, \forall m$, and $\eta_{k, \mathcal{C}_m} = \eta_k$.

²In practical scenarios, channel statistics can be acquired through various methods, including time-averaged estimation, user feedback, model-based predictions, and pilot signals. Moreover, machine learning techniques are increasingly being used to acquire channel statistics from historical data and user context [26].

2) *CF-mMIMO with Fully Distributed Beamforming:* In this case, the beamforming can be done locally at each AP without CSI exchange with other APs. This makes the network truly distributed. In particular, each BBH at each AP utilizes its own local channel estimates to generate a ZF precoder. CF-mMIMO with distributed beamforming corresponds to the case when there are M beamforming clusters, i.e., $C = M$, $\mathcal{C}_m = m, \forall m$, with cardinality 1, each includes $\mathcal{U}_m = \mathcal{K}_m$ users. Also, in this case power control coefficient for user k is $\eta_{k, \mathcal{C}_m} = \eta_{k, m}$. In this case, each AP can only mitigate its own interference, but not interference from other APs. Note that this can be seen as a particular CF-mMIMO configuration with pure UC clustering and fully distributed beamforming which does not require any CSI to be exchanged between BBHs.

B. Fronthaul Requirements

In a CF-mMIMO system with BBH-BBL operation, precoding weights are calculated at BBH. Then precoding weights and user data are sent to BBL via fronthaul links. We consider packed-based evolved CPRI (eCPRI) for the fronthaul transmission. More specifically, fronthaul requirement of m -th AP for downlink data transmission in the considered CF-mMIMO system with BBH-BBL operation can be calculated as

$$\text{FH}_{m, \text{data}} = \frac{\log_2(M_{\text{order}}) \bar{N} K_m N_{\text{subcarrier}} N_{\text{OFDM}}}{\text{eCPR}_{\text{eff}} \text{delay}_{\text{data}}}, \quad (23)$$

where M_{order} is the modulation order, $N_{\text{subcarrier}}$ denotes the number of OFDM subcarrier, and $\text{delay}_{\text{data}}$ and eCPR_{eff} are constant parameters. Moreover, the required fronthaul capacity for beamforming weights is given by

$$\text{FH}_{m, \text{BF}} = \frac{2L \bar{N} K_m N_{\text{bits}} N_{\text{Gran}}}{\text{eCPR}_{\text{eff}} \text{delay}_{\text{precoder}}}, \quad (24)$$

where N_{bits} is the number of quantization bits and N_{Gran} is the beamforming granularity. More specifically, if we denote the number of subcarriers grouped under one precoding operation as N_{Group} , then $N_{\text{Gran}} = \frac{N_{\text{subcarrier}}}{N_{\text{Group}}}$. Based on (23) and (24), fronthaul requirement scales with the number of users that each AP serves and also the number of data streams to be sent to each user. Accordingly, in the proposed CF-mMIMO system, we constrain the downlink traffic bandwidth to be fronthauled by limiting the number of users that each AP serves and the number of independent downlink data streams sent to each user, i.e.,

- Each BBH m only needs to send data and precoding matrix of $K_m \leq K$ users to its BBL through fronthaul link (this is in contrast with the conventional CF-mMIMO system, which requires fronthauled information of all K users).
- We suppose \bar{N} takes an integer value from 1 to N . Therefore, each fronthaul link needs to support $\bar{N} \leq N$ downlink data streams per user.

On the other hand, a higher modulation order, M_{order} , is essential to achieve the high data rates. However, from (23), fronthaul requirement for data transmission increases with M_{order} , thus, there is a trade-off between the SE and fronthaul requirement. From the information-theoretic perspective, modulation-constrained achievable information rate, \mathcal{R}_{mo} , is bounded as $\mathcal{R}_{\text{mo}} < \bar{\mathcal{C}}$, where $\bar{\mathcal{C}}$ is the AWGN channel

capacity. Besides, \mathcal{R}_{mo} cannot be greater than the entropy of the corresponding constellation, i.e., $\mathcal{R}_{\text{mo}} < \log_2(M_{\text{order}})$. Thus, \mathcal{R}_{mo} can be upper-bounded as

$$\mathcal{R}_{\text{mo}} \leq \min(\bar{C}, \log_2(M_{\text{order}})). \quad (25)$$

At high signal-to-noise ratio (SNR), \mathcal{R}_{mo} approaches the constellation entropy $\log_2(M_{\text{order}})$ and is independent of the SNR, so that the upper bound in (25) is tight at high SNR [27].

Accordingly, from (23), (24), and (25), the per-AP fronthaul capacity constraints can be written as

$$\text{FH}_{m,\text{data}} + \text{FH}_{m,\text{BF}} = \bar{N}K_m(\alpha_1 \log_2(M_{\text{order}}) + \alpha_2) \leq \text{FH}_{\text{max}}, \quad \forall m, \quad (26)$$

and

$$R_k \leq \log_2(M_{\text{order}}), \quad \forall k, \quad (27)$$

where FH_{max} is the per-AP maximum fronthaul constraint for downlink data transmission and beamforming weights, $\alpha_1 \triangleq \frac{N_{\text{subcarrier}} N_{\text{OFDM}}}{e\text{CPR}_{\text{eff}} \text{delay}_{\text{data}}}$, and $\alpha_2 \triangleq \frac{2LN_{\text{bits}} N_{\text{Gran}}}{e\text{CPR}_{\text{eff}} \text{delay}_{\text{precoder}}}$.

IV. JOINT USER ASSOCIATION AND POWER ALLOCATION

We aim to optimize UC clustering and downlink transmit powers for the maximization of the system sum SE, subject to per-AP fronthaul capacity and maximum transmit power constraints. We would like to highlight that the presence of multiple antennas at users in the CF-mMIMO system plays a critical role in the optimization process. In particular, multi-antenna users enhance SINR and detection through spatial diversity and multiplexing, influencing resource allocation via the effective channel gain matrix. On the other hand, multi-antenna configurations increase fronthaul usage, tightening constraints on the number of users served. Our optimization framework accounts for these interactions by incorporating fronthaul-constrained rate limits, ensuring efficient resource allocation under practical constraints. Accordingly, in what follows we formulate joint user association and power allocation for a given large-scale fading coherence time.

A. Sum-SE Maximization

With (8) the expected transmit signal power from AP m is given by

$$\mathbb{E}\{\mathbf{s}_m^H \mathbf{s}_m\} = P \sum_{k \in \mathcal{K}_m} \eta_{k,C_m} \text{tr}(\mathbb{E}\{\mathbf{Q}_{mk} \mathbf{Q}_{mk}^H\}). \quad (28)$$

Therefore, the per-AP power constraint can be written as

$$\sum_{k \in \mathcal{K}_m} \eta_{k,C_m} \text{tr}(\mathbb{E}\{\mathbf{Q}_{mk} \mathbf{Q}_{mk}^H\}) \leq 1. \quad (29)$$

Now, let $\boldsymbol{\eta}$ denote the set of all power control coefficients $\boldsymbol{\eta} \triangleq \{\eta_{k,C_m} : k = 1, \dots, K; m = 1, \dots, M\}$. Recall that for the given AP n and AP m in the same CB cluster, we have $\mathcal{C}_n = \mathcal{C}_m$ and $\eta_{k,C_m} = \eta_{k,C_n} \forall k$. For convenience, let $\mathcal{K} \triangleq \{\bigcup_{m=1}^M \mathcal{K}_m, m = 1, \dots, M\}$ denote the UC clustering control variable. Now, for the given CB clustering, the sum-SE maximization problem can be formulated as

$$\max_{\boldsymbol{\eta}, \mathcal{K}} \sum_{k=1}^K R_k(\boldsymbol{\eta}, \mathcal{K}) \quad (30a)$$

$$\text{st. } \eta_{k,C_m} \geq 0, \quad \forall m, k, \quad (30b)$$

$$R_k(\boldsymbol{\eta}, \mathcal{K}) \leq \log_2(M_{\text{order}}), \quad \forall k, \quad (30c)$$

$$\bar{N}K_m(\alpha_1 \log_2(M_{\text{order}}) + \alpha_2) \leq \text{FH}_{\text{max}}, \quad \forall m, \quad (30d)$$

$$\sum_{k \in \mathcal{K}_m} \eta_{k,C_m} \text{tr}(\mathbb{E}\{\mathbf{Q}_{mk} \mathbf{Q}_{mk}^H\}) \leq 1, \quad \forall m. \quad (30e)$$

Optimization problem (30) is obviously nonconvex due to i) the presence of unknown optimization variables \mathcal{K}_m and η_{k,C_m} , $m \in \{1, \dots, M\}$, $k \in \{1, \dots, K\}$, appearing as products in $R_k(\boldsymbol{\eta}, \mathcal{K})$ ii) beamforming matrix \mathbf{Q} is a non-convex function of \mathcal{K} . Therefore, the joint optimization of $\boldsymbol{\eta}$ and \mathcal{K} cannot be implemented in a complexity-efficient way and hence, we separate the optimization variables and solve the corresponding sub-problems with time-efficient algorithms.

B. Power Allocation Optimization Given User Association

The power allocation problem with fixed UC association \mathcal{K} is expressed as

$$\max_{\boldsymbol{\eta}} \sum_{k=1}^K R_k(\boldsymbol{\eta}) \quad (31a)$$

$$\text{st. } \eta_{k,C_m} \geq 0, \quad \forall m, k, \quad (31b)$$

$$R_k(\boldsymbol{\eta}) \leq \log_2(M_{\text{order}}), \quad \forall k, \quad (31c)$$

$$\sum_{k \in \mathcal{K}_m} \eta_{k,C_m} \text{tr}(\mathbb{E}\{\mathbf{Q}_{mk} \mathbf{Q}_{mk}^H\}) \leq 1, \quad \forall m. \quad (31d)$$

This problem is non-convex due to the non-convex objective function (31a) and non-convex constraint (31c), which makes its solution difficult. Thus, we resort to sequential optimization framework, also known as MM approach. By using this iterative framework, we can reformulate the original non-convex problem into a series of auxiliary convex subproblems that can be easily solved by algorithms that have low computational complexity and their solutions converge to a locally optimal solution of the original problem [28]. The proposed MM strategy, at each iteration, solves an auxiliary problem whose objective function is a lower-bound of Problem (31a). Such a lower bound must fulfill the following criteria: it must be equal to the original function (31a); its gradient and of the original objective function (31) must be equal at the point $\boldsymbol{\eta}_k$, which is updated at each algorithm's iteration. To this end, we need to derive a proper lower-bound of the objective function of (31). Using the fact that $\det(\mathbf{I}_M + \mathbf{A}_1 \mathbf{A}_2) = \det(\mathbf{I}_N + \mathbf{A}_2 \mathbf{A}_1)$, where \mathbf{A}_1 and \mathbf{A}_2 are matrices of size $M \times N$ and $N \times M$, respectively, the SE of the user k , $k = 1, \dots, K$, can be rewritten as

$$R_k(\tilde{\boldsymbol{\eta}}) = (1 - \tau_u / \tau_c) [g(\boldsymbol{\Omega}_k(\tilde{\boldsymbol{\eta}})) - g(\boldsymbol{\Xi}_k(\tilde{\boldsymbol{\eta}}))], \quad (32)$$

where $\tilde{\boldsymbol{\eta}} \triangleq \{\tilde{\eta}_{k',C_m,C_n} : k' = 1, \dots, K; m = 1, \dots, M, n = 1, \dots, M\}$, $\tilde{\eta}_{k',C_m,C_n} = \eta_{k',C_m}^{1/2} \eta_{k',C_n}^{1/2}$, $g(\cdot) \triangleq \log_2|\cdot|$,

$$\boldsymbol{\Omega}_k(\tilde{\boldsymbol{\eta}}) = P \sum_{k'=1}^K \sum_{m \in \mathcal{M}_{k'}} \sum_{n \in \mathcal{M}_{k'}} \tilde{\eta}_{k',C_m,C_n} \mathbb{E}\{\mathbf{G}_{mk}^H \mathbf{Q}_{mk'} \times \mathbf{Q}_{nk'}^H \mathbf{G}_{nk}\} + \sigma^2 \mathbf{I}_N, \quad (33)$$

and

$$\begin{aligned} \boldsymbol{\Xi}_k(\tilde{\boldsymbol{\eta}}) = & P \sum_{k'=1}^K \sum_{m \in \mathcal{M}_{k'}} \sum_{n \in \mathcal{M}_{k'}} \tilde{\eta}_{k',C_m,C_n} \mathbb{E}\{\mathbf{G}_{mk}^H \mathbf{Q}_{mk'} \times \\ & \mathbf{Q}_{nk'}^H \mathbf{G}_{nk}\} - P \sum_{m \in \mathcal{M}_k} \sum_{n \in \mathcal{M}_k} \tilde{\eta}_{k,C_m,C_n} \mathbb{E}\{\mathbf{G}_{mk}^H \mathbf{Q}_{mk} \times \\ & \mathbf{Q}_{nk}^H \mathbf{G}_{nk}\} + \sigma^2 \mathbf{I}_N. \end{aligned} \quad (34)$$

Each term of the sum in both $\boldsymbol{\Omega}_k(\tilde{\boldsymbol{\eta}})$ and $\boldsymbol{\Xi}_k(\tilde{\boldsymbol{\eta}})$ in (33) and (34), respectively, is concave. In addition, the summation preserves concavity and the function $\log_2|\cdot|$ is matrix-

increasing. As a result, $g(\mathbf{\Omega}_k(\tilde{\boldsymbol{\eta}}))$ and $g(\mathbf{\Xi}_k(\tilde{\boldsymbol{\eta}}))$ in (32) are concave functions. Problem (31) is equivalent to

$$\min_{\boldsymbol{\eta}, \tilde{\boldsymbol{\eta}}} - \sum_{k=1}^K R_k(\tilde{\boldsymbol{\eta}}) \quad (35a)$$

$$\text{st. } \eta_{k,c_m} \geq 0, \quad \forall m, k, \quad (35b)$$

$$R_k(\tilde{\boldsymbol{\eta}}) \leq \log_2(M_{\text{order}}), \quad \forall k, \quad (35c)$$

$$\sum_{k \in \mathcal{K}_m} \eta_{k,c_m} \text{tr}(\mathbb{E}\{\mathbf{Q}_{mk} \mathbf{Q}_{mk}^H\}) \leq 1, \quad \forall m, \quad (35d)$$

$$\tilde{\eta}_{k',c_m,c_n}^2 = \eta_{k',c_m} \eta_{k',c_n}, \quad \forall k', m, n. \quad (35e)$$

We replace constraint (35e) by

$$\tilde{\eta}_{k',c_m,c_n}^2 \leq \eta_{k',c_m} \eta_{k',c_n}, \quad (36)$$

$$\tilde{\eta}_{k',c_m,c_n}^2 \geq \eta_{k',c_m} \eta_{k',c_n}. \quad (37)$$

From (36), it is true that (37) is equivalent to

$$T(\boldsymbol{\eta}, \tilde{\boldsymbol{\eta}}) = \sum_{k'=1}^K \sum_{m \in \mathcal{M}_{k'}} \sum_{n \in \mathcal{M}_{k'}} (\eta_{k',c_m} \eta_{k',c_n} - \tilde{\eta}_{k',c_m,c_n}^2) \leq 0. \quad (38)$$

Accordingly, problem (35) can be written in a more tractable form as

$$\min_{\boldsymbol{\eta}, \tilde{\boldsymbol{\eta}}} - \sum_{k=1}^K R_k(\tilde{\boldsymbol{\eta}}) \quad (39a)$$

$$\text{st. } \eta_{k,c_m} \geq 0, \quad \forall m, k, \quad (39b)$$

$$R_k(\tilde{\boldsymbol{\eta}}) \leq \log_2(M_{\text{order}}), \quad \forall k, \quad (39c)$$

$$\sum_{k \in \mathcal{K}_m} \eta_{k,c_m} \text{tr}(\mathbb{E}\{\mathbf{Q}_{mk} \mathbf{Q}_{mk}^H\}) \leq 1, \quad \forall m, \quad (39d)$$

$$\tilde{\eta}_{k',c_m,c_n}^2 \leq \eta_{k',c_m} \eta_{k',c_n}, \quad \forall k', m, n, \quad (39e)$$

$$T(\boldsymbol{\eta}, \tilde{\boldsymbol{\eta}}) \leq 0. \quad (39f)$$

Now, consider the following optimization problem

$$\min_{\boldsymbol{\eta}, \tilde{\boldsymbol{\eta}}} \mathcal{L}(\boldsymbol{\eta}, \tilde{\boldsymbol{\eta}}) \quad (40a)$$

$$\text{st. } \eta_{k,c_m} \geq 0, \quad \forall m, k, \quad (40b)$$

$$R_k(\tilde{\boldsymbol{\eta}}) \leq \log_2(M_{\text{order}}) \quad \forall k, \quad (40c)$$

$$\sum_{k \in \mathcal{K}_m} \eta_{k,c_m} \text{tr}(\mathbb{E}\{\mathbf{Q}_{mk} \mathbf{Q}_{mk}^H\}) \leq 1, \quad \forall m, \quad (40d)$$

$$\tilde{\eta}_{k',c_m,c_n}^2 \leq \eta_{k',c_m} \eta_{k',c_n}, \quad \forall k', m, n, \quad (40e)$$

where $\mathcal{L}(\boldsymbol{\eta}, \tilde{\boldsymbol{\eta}}) \triangleq -\sum_{k=1}^K R_k(\tilde{\boldsymbol{\eta}}) + \lambda T(\boldsymbol{\eta}, \tilde{\boldsymbol{\eta}})$ is the Lagrangian of (39) and λ is the Lagrangian multiplier corresponding to constraint (39f).

Proposition 2. The value T_λ of T at the solution of (40) corresponding to λ converges to 0 as $\lambda \rightarrow +\infty$. Moreover, problem (39) has strong duality, such that

$$\min_{\{\boldsymbol{\eta}, \tilde{\boldsymbol{\eta}}\} \in \mathcal{F}} - \sum_{k=1}^K R_k(\tilde{\boldsymbol{\eta}}) = \sup_{\lambda \geq 0} \min_{\{\boldsymbol{\eta}, \tilde{\boldsymbol{\eta}}\} \in \tilde{\mathcal{F}}} \mathcal{L}(\boldsymbol{\eta}, \tilde{\boldsymbol{\eta}}), \quad (41)$$

where \mathcal{F} and $\tilde{\mathcal{F}}$ are feasible sets defined as $\mathcal{F} \triangleq \{(39b), (39c), (39d), (39e), (39f)\}$ and $\tilde{\mathcal{F}} \triangleq \mathcal{F} \setminus (39f)$, respectively. Therefore, at the optimum solution $\lambda^* \geq 0$ of (41), problems (39) and (40) are equivalent.

Proof. The proof follows [29]. \square

Attaining the optimal solution for problem (39) necessitates T_λ to be zero, which occurs when $\lambda \rightarrow +\infty$, as indicated by Proposition 2. However, for practice implementation, it is sufficient to consider $T_\lambda \leq \varepsilon$, for some small value of ε with a sufficiently large value of λ [29], [30].

Algorithm 1 Power Allocation Optimization Given User Association

- 1: Set $\iota = 0$ and choose any feasible $\boldsymbol{\eta}^{(\iota)} = \boldsymbol{\eta}^{(0)}$ and $\tilde{\boldsymbol{\eta}}^{(\iota)} = \tilde{\boldsymbol{\eta}}^{(0)}$.
 - 2: **repeat**
 - 3: Perform power allocation optimization (48): $\boldsymbol{\eta}^{(\iota+1)} = \text{Optimize}(\boldsymbol{\eta}^{(\iota)})$.
 - 4: Increase the super-iteration index: $\iota \leftarrow \iota + 1$.
 - 5: **until** convergence
-

We note that the objective function (40) is still non-convex and difficult to handle. Therefore, we substitute it with a tractable upper bound. Recall the fact that the convex function $-g(\cdot) = -\log_2(|\cdot|)$ is lower bounded by its first-order Taylor expansion at any local points [31]. Accordingly, we can derive as

$$\begin{aligned} R_k(\tilde{\boldsymbol{\eta}}) &= g(\mathbf{\Omega}_k(\tilde{\boldsymbol{\eta}})) - g(\mathbf{\Xi}_k(\tilde{\boldsymbol{\eta}})) \\ &\geq g(\mathbf{\Omega}_k(\tilde{\boldsymbol{\eta}})) - g(\mathbf{\Xi}_k^{(0)}(\tilde{\boldsymbol{\eta}})) \\ &\quad - \text{tr} \left(\left(\mathbf{\Xi}_k^{(0)} \right)^{-1} \left(\mathbf{\Xi}_k(\tilde{\boldsymbol{\eta}}) - \mathbf{\Xi}_k^{(0)} \right) \right) \triangleq \tilde{R}_k^L(\tilde{\boldsymbol{\eta}}), \end{aligned} \quad (42)$$

where $\mathbf{\Xi}_k^{(0)} = \mathbf{\Xi}_k(\tilde{\boldsymbol{\eta}}^{(0)})$. Moreover, the convex upper bounds of T can be written as

$$\begin{aligned} \tilde{T}^U(\boldsymbol{\eta}, \tilde{\boldsymbol{\eta}}) &\triangleq \sum_{k'=1}^K \sum_{m \in \mathcal{M}_{k'}} \sum_{n \in \mathcal{M}_{k'}} 0.25 [(\eta_{k',c_m} + \eta_{k',c_n})^2 \\ &\quad - 2(\eta_{k',c_m}^{(0)} - \eta_{k',c_n}^{(0)})(\eta_{k',c_m} - \eta_{k',c_n}) + (\eta_{k',c_m}^{(0)} - \eta_{k',c_n}^{(0)})^2 \\ &\quad - 8\tilde{\eta}_{k',c_m,c_n}^{(0)} \tilde{\eta}_{k',c_m,c_n} + 4(\tilde{\eta}_{k',c_m,c_n}^{(0)})^2], \end{aligned} \quad (43)$$

where we have used the fact that for given $a \geq 0$ and $b \geq 0$ $ab \leq 0.25[(a+b)^2 - 2(a^{(0)} - b^{(0)})(a-b) + (a^{(0)} - b^{(0)})^2]$. (44)

Moreover, the constraints (40c) and (40e) are still non-convex and needs to be approximated by a convex upper bound. Following the fact that the first-order Taylor approximation is a global upper estimator of a concave function, we have

$$\begin{aligned} R_k(\tilde{\boldsymbol{\eta}}) &\leq g(\mathbf{\Omega}_k^{(0)}) + \text{tr} \left(\left(\mathbf{\Omega}_k^{(0)} \right)^{-1} \left(\mathbf{\Omega}_k(\tilde{\boldsymbol{\eta}}) - \mathbf{\Omega}_k^{(0)} \right) \right) \\ &\quad - g(\mathbf{\Xi}_k(\tilde{\boldsymbol{\eta}})) \triangleq \tilde{R}_k^U(\tilde{\boldsymbol{\eta}}), \end{aligned} \quad (45)$$

where $\mathbf{\Omega}_k^{(0)} = \mathbf{\Omega}_k(\tilde{\boldsymbol{\eta}}^{(0)})$. In addition, since $\forall a \geq 0$ and $b \geq 0$ we have [32],

$$\begin{aligned} -ab &\leq 0.25[(a-b)^2 \\ &\quad - 2(a^{(n)} + b^{(n)})(a+b) + (a^{(n)} + b^{(n)})^2], \end{aligned} \quad (46)$$

the convex upper bounds of (40e) can be expressed as

$$\begin{aligned} \tilde{\eta}_{k',c_m,c_n}^2 &+ 0.25[(\eta_{k',c_m}^{(n)} - \eta_{k',c_n}^{(n)})^2 - 2(\eta_{k',c_m}^{(n)} + \eta_{k',c_n}^{(n)}) \times \\ &\quad (\eta_{k',c_m} + \eta_{k',c_n}) + (\eta_{k',c_m}^{(n)} + \eta_{k',c_n}^{(n)})^2] \leq 0. \end{aligned} \quad (47)$$

We are now ready to handle the Problem (39) by the sequential optimization framework. More specifically, at iteration $(\iota+1)$, for the given points $\boldsymbol{\eta}^{(\iota)}, \tilde{\boldsymbol{\eta}}^{(\iota)}$, problem (40) can finally be approximated by

$$\min_{\boldsymbol{\eta}, \tilde{\boldsymbol{\eta}}} \hat{\mathcal{L}}(\boldsymbol{\eta}, \tilde{\boldsymbol{\eta}}) \quad (48a)$$

$$\text{st. } \eta_{k,c_m} \geq 0, \quad \forall m, k, \quad (48b)$$

$$\tilde{R}_k^U(\tilde{\boldsymbol{\eta}}) \leq \log_2(M_{\text{order}}), \quad \forall k, \quad (48c)$$

$$\sum_{k \in \mathcal{K}_m} \eta_{k,c_m} \text{tr}(\mathbb{E}\{\mathbf{Q}_{mk} \mathbf{Q}_{mk}^H\}) \leq 1, \quad \forall m, \quad (48d)$$

Algorithm 2 User Association Given Power Allocation

- 1: Let \mathcal{K}_m be the set of users associated with AP m . Initialize $\mathcal{K}_m = \emptyset, m = 1, \dots, M$, and set K_{\max} as maximum number of users that can associate with each AP based on (50).
 - 2: **for** $m = 1 : M$ **do**
 - 3: Let, $\beta_{m,m^{(1)}}, \beta_{m,m^{(2)}}, \dots, \beta_{m,m^{(K)}}$, where $m^{(k)} \in \{1, \dots, K\}$, be the ordered channel gain (large-scale fading coefficient) from AP m to user $k, k = 1, \dots, K$, in descending order $\beta_{m,m^{(1)}} \geq \beta_{m,m^{(2)}} \geq \dots \geq \beta_{m,m^{(K)}}$.
 - 4: AP m is associated with $K_{\max} \leq K$ users corresponding to the K_{\max} largest large-scale fading coefficients. That is, \mathcal{K}_m is set as $\mathcal{K}_m = \{m^{(1)}, \dots, m^{(K_{\max})}\}$.
 - 5: **end for**
-

$$\tilde{\eta}_{k',c_m,c_n}^2 + 0.25[(\eta_{k',c_m} - \eta_{k',c_n})^2 - 2(\eta_{k',c_m}^{(n)} + \eta_{k',c_n}^{(n)}) \times (\eta_{k',c_m} + \eta_{k',c_n}) + (\eta_{k',c_m}^{(n)} + \eta_{k',c_n}^{(n)})^2] \leq 0, \quad \forall k', m, n, \quad (48e)$$

where

$$\begin{aligned} \hat{\mathcal{L}}(\boldsymbol{\eta}, \tilde{\boldsymbol{\eta}}) = & - \sum_{k=1}^K \tilde{R}_k^L(\tilde{\boldsymbol{\eta}}) + \lambda \sum_{k'=1}^K \sum_{m \in \mathcal{M}_k} \sum_{n \in \mathcal{M}_k} 0.25 \times \\ & [(\eta_{k',c_m} + \eta_{k',c_n})^2 - 2(\eta_{k',c_m}^{(0)} - \eta_{k',c_n}^{(0)}) (\eta_{k',c_m} - \eta_{k',c_n}) + \\ & (\eta_{k',c_m}^{(0)} - \eta_{k',c_n}^{(0)})^2 - 8\tilde{\eta}_{k',c_m,c_n}^{(0)} \tilde{\eta}_{k',c_m,c_n} + 4(\tilde{\eta}_{k',c_m,c_n}^{(0)})^2]. \end{aligned} \quad (49)$$

The objective function in Problem (48) is convex and the constraints are also affine, and hence can be solved using standard convex optimization theory. The resulting sequential optimization algorithm for solving (48) is formulated in Algorithm 1³. Choosing any feasible points $\{\boldsymbol{\eta}, \tilde{\boldsymbol{\eta}}\} \in \hat{\mathcal{F}}$ we solve power allocation problem (48) to obtain its optimal solution $\boldsymbol{\eta}^*, \tilde{\boldsymbol{\eta}}^*$ which then be used as the initial points in the next iteration. The process being iterated until an accuracy level of ε is attained. Using [29, Proposition 2] it can be readily showed that Algorithm 1 will converge to a stationary point, i.e., a Fritz John solution, of problem (48) (hence (31)).

C. User Association Given Power Allocation

Thus far in this section, we dealt with the power allocation design under fronthaul and per-AP transmit power constraint for any given fixed user association. We now propose a heuristic user association algorithm for the given power allocation. The fronthaul constraint (30d) poses an upper bound on the number of users that can associate with each AP m , K_m , by K_{\max} as

$$\begin{aligned} \bar{N} K_m (\alpha_1 \log_2(M_{\text{order}}) + \alpha_2) & \leq \text{FH}_{\max} \\ K_m & \leq \left\lfloor \frac{\text{FH}_{\max}}{\bar{N} (\alpha_1 \log_2(M_{\text{order}}) + \alpha_2)} \right\rfloor \triangleq K_{\max}, \end{aligned} \quad (50)$$

where $\lfloor \cdot \rfloor$ is the floor function.

In the proposed user association scheme each AP sorts the channel gains in descending order and independently selects K_{\max} users with the strongest channel gains. The proposed user association scheme is described in Algorithm 2.

³Although this work presents results for an i.i.d. fading channel model, the proposed optimization framework in Algorithm 1 is general and can be extended to accommodate more realistic channel models as required.

D. Computational Complexity

Here, we compare the complexity of the beamforming design and power allocation for the UC generalized ZF-based CF-mMIMO system. The details of the computational complexity calculation are presented in Appendix A, where complexity is quantified in terms of the number of real floating-point operations (flops).

1) *Computational Complexity of Beamforming Design:* The total flop count for the beamforming calculation of CB cluster \mathcal{C}_m is $\varpi = NU_m + 24NL^2U_mC_m^2 + 56N^2LU_m^2C_m + 54N^3U_m^3$. It is observed that the computational complexity of the generalized CF-mMIMO system at each AP m depends on the number of APs in its corresponding CB cluster, C_m , with $1 \leq C_m \leq M$, and the cardinality of its associated user set \mathcal{U}_m , U_m , with $1 \leq U_m \leq K$. The corresponding computational complexity of fully centralized beamforming design (fully distributed beamforming design) can be obtained by replacing C_m and U_m in ϖ with M and K (1 and K_{\max}), respectively.

2) *Computational Complexity of Power Allocation:* The computational complexity of power allocation for the generalized CF-mMIMO system with C CB is given by $\mathcal{O}(\iota\sqrt{M+K+KC^2}(KC(2C+1)+M+K)(KC(C+1))^2)$. The CF-mMIMO system with fully distributed beamforming design exhibits the highest power allocation computation complexity. This is because its corresponding problem involves computing up to MK power allocation coefficients.

We emphasize that the power allocation optimization in Algorithm 1 is scalable, with scalability ensured through careful consideration of computational complexity, adaptability to various system setups, and fronthaul constraints. Similarly, the proposed user association in Algorithm 2 is simple, low-complexity, and efficient. Both algorithms rely on statistical CSI, requiring only large-scale channel statistics, which change slowly over time and remain constant across frequencies. Unlike small-scale fading coefficients, which vary rapidly, large-scale fading evolves more gradually. Therefore, when the system remains static (with unchanged users) for extended periods, power allocation and user association only need to be performed once and can be applied to all subcarriers across multiple frame durations. This significantly reduces the need for frequent recalculations, while beamforming, based on instantaneous CSI, remains the dominant factor in computational complexity. Among the considered beamforming designs, the distributed design has the lowest complexity in calculating beamforming matrices and the least fronthaul overhead for CSI exchange, while the centralized design has the highest computational complexity and fronthaul overhead.

V. NUMERICAL RESULTS

We consider a CF-mMIMO system where the APs and users are randomly distributed in a square of $1 \times 1 \text{ km}^2$, whose edges are wrapped around to avoid the boundary effects. Each AP can serve up to K_{\max} users out of a set of K users. The value of parameter K_{\max} depends on the system and fronthaul parameters and is determined based on (50).

TABLE I: Fronthaul parameters for the simulation

Parameter	Value	Parameter	Value
Number of OFDM subcarriers, $N_{\text{subcarrier}}$	3264	N_{Gran}	136
eCPR_{eff}	0.85	$\text{delay}_{\text{precoder}}(\text{delay}_{\text{data}})$	$2 \times 10^{-4} (5 \times 10^{-4})$ s
Number of OFDM symbols, N_{OFDM}	14 sym	Number of quantization bits, N_{bits}	16

A. Simulation Setup and Parameters

The large-scale fading coefficient β_{mk} includes the path loss and shadow fading, according to

$$\beta_{mk} = 10^{\frac{\text{PL}_{mk}}{10}} 10^{\frac{\sigma_{sh} y_{mk}}{10}}, \quad (51)$$

where the second term models the shadow fading with standard deviation $\sigma_{sh} = 4$ dB and $y_{mk} \sim \mathcal{CN}(0, 1)$, while PL_{mk} (in dB) is calculated as

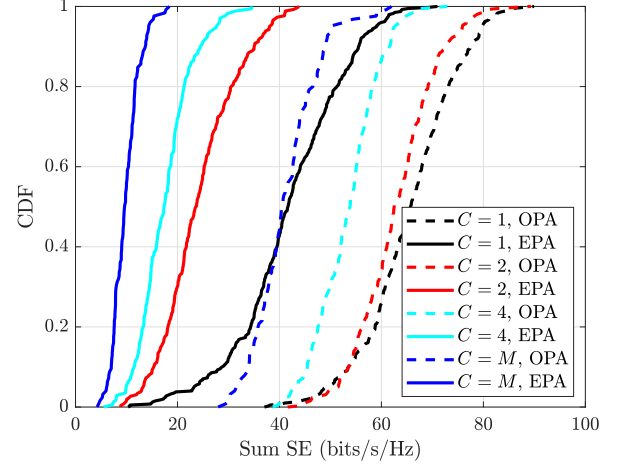
$$\text{PL}_{mk} = \begin{cases} -L - 35 \log_{10}(d_{mk}), & d_{mk} > d_1, \\ -L - 15 \log_{10}(d_1) - 20 \log_{10}(d_{mk}), & d_0 < d_{mk} \leq d_1, \\ -L - 15 \log_{10}(d_1) - 20 \log_{10}(d_0), & d_{mk} \leq d_0, \end{cases} \quad (52)$$

with $L = 46.3 + 33.9 \log_{10}(f) - 13.82 \log_{10}(h_{\text{AP}}) - (1.1 \log_{10}(f) - 0.7)h_{\text{U}} + (1.56 \log_{10}(f) - 0.8)$. In addition, f is the carrier frequency (in MHz), d_{mk} denotes the distance between AP m and user k (in m), h_{AP} and h_{U} are the antenna heights at the AP and at the user (in m), respectively. Here, we choose $d_0 = 10$ m, $d_1 = 50$ m, $h_{\text{AP}} = 15$ m and $h_{\text{U}} = 1.65$ m. These parameters resemble those in [1]. The maximum transmit power for training pilot sequences and each AP is 100 mW, while the noise power is $\sigma_n^2 = -92$ dBm. In what follows, unless otherwise stated, we choose the fronthaul parameters summarized in Table I, and set $M_{\text{order}} = 2^9$. In addition, we consider 100 MHz bandwidth with 30 kHz subcarrier spacing which corresponds to $N_{\text{subcarrier}} = 3264$ as in Table I. Moreover, we select $\tau_c = 2000$ samples, corresponding to a coherence bandwidth of 200 kHz and a coherence time of 10 ms.

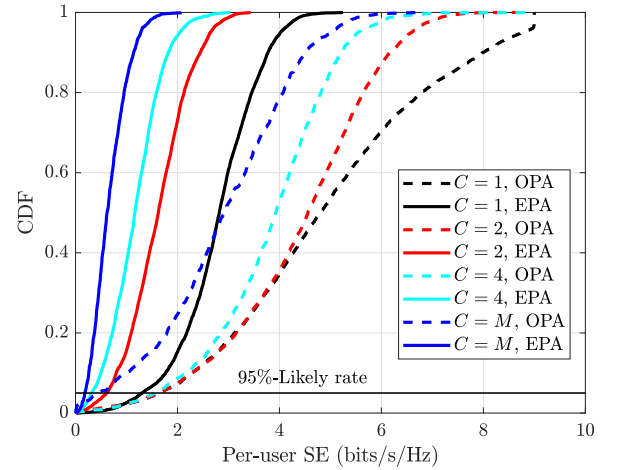
We compare the performance of the following cases:

- $C = 1$: In this case there is 1 CB cluster consisting of all the APs in the network, which can be considered as a CF-mMIMO system with fully centralized CB.
- $C = 2$: In this case, APs are divided into $C = 2$ disjoint CB clusters.
- $C = 4$: In this case, APs are divided into $C = 4$ disjoint CB clusters.
- $C = M$: In this case, we have $C = M$ CB clusters with cardinality 1. This case corresponds to the CF-mMIMO system with fully distributed beamforming.

For CB clustering, we consider a simple distributed CB architecture where APs are divided into C disjoint CB clusters based on their geographical positions. Moreover, the notations OPA and EPA describe the performance achieved by the proposed power allocation Algorithm 1 and low-complexity heuristic power control [16], as outlined as follows, respectively. With (8) and (29), the per-AP power constraint for AP m in CB cluster \mathcal{C}_m can be written as $\sum_{k \in \mathcal{K}_m} \eta_{k, \mathcal{C}_m} \text{tr}(\mathbb{E}\{\mathbf{Q}_{mk} \mathbf{Q}_{mk}^H\}) \leq 1$. Accordingly, in EPA, the power coefficient used by AP m for transmission to user



(a) CDF of the sum SE



(b) CDF of the per-user SE

Fig. 3: Comparison between the sum SE and per-user SE achieved by the proposed power allocation and user association and baseline schemes for different number of CB clusters. Here, $M = 10$, $N = 2$, $\bar{N} = 1$, $\text{FH}_{\text{max}} = 14$ Gbps, and $L = 22$.

k is calculated as

$$\eta_{k, \mathcal{C}_m} = \frac{1}{\max_m (\sum_{k \in \mathcal{K}_m} \delta_{mk})}, \quad \forall k \in \mathcal{K}_m, m \in \mathcal{C}_m, \quad (53)$$

where $\delta_{mk} \triangleq \text{tr}(\mathbb{E}\{\mathbf{Q}_{mk} \mathbf{Q}_{mk}^H\})$.

B. Results and Discussions

1) *Power Allocation and User Association*: In Fig. 3 we evaluate the performance of the proposed power allocation and user association in the fronthaul-aware downlink CF-mMIMO system. Numerical results lead to the following conclusions.

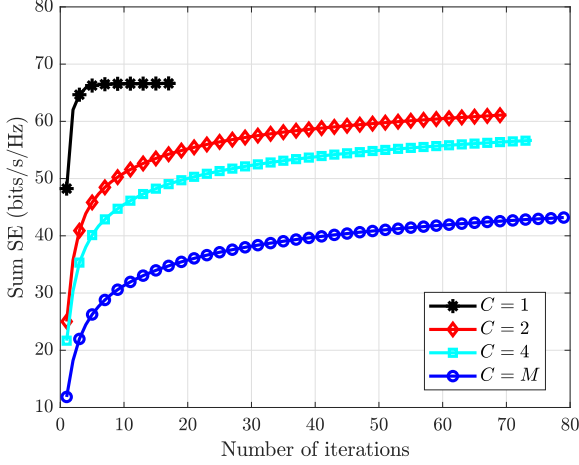


Fig. 4: Convergence of the proposed Algorithm 1, where $M = 10$, $K = 15$, $N = 2$, $\bar{N} = 1$, $L = 22$, and $\text{FH}_{\max} = 14$ Gbps.

- The proposed power allocation and user association solution resulting from the optimization Algorithm 1, yields significant sum-SE and per-user SE performance increase against EPA for different cases. More specifically, it provides sum-SE performance gains of up to 59%, 173%, 252%, and 312%, over EPA for $C = 1$, $C = 2$, $C = 4$, and $C = M$ cases, respectively, which highlights the advantage of our power optimization solution over heuristic ones.
- It is observed that the performance gain is minimal when $C = 1$, whereas it is maximal when $C = M$. The reason is twofold: 1) primarily due to the fact that when $C = 1$, the fully centralized CB handles all interference cancellation, leaving little room for further improvement in sum-SE performance. However, for larger values of C , the residual interference can be effectively mitigated through a carefully designed power allocation scheme, leading to significant performance enhancements when power allocation is optimized; 2) secondarily because when power allocation is optimized, increasing the number of CB clusters provides a greater flexibility. In fact, in the system with $C = 1$ CB cluster, we optimize up to K power allocation coefficients. However, in the system with C CB clusters, we can optimize the sum SE over CK transmit powers. Therefore, the solution space is expanding by increasing the number of CB clusters.
- The sum-SE performance gap between $C = M$ and $C = 1$, decreases with OPA. For example, the sum-SE performance loss of $C = M$ case with respect to $C = 1$ case is 75% and 38% under EPA and OPA strategies, respectively.
- From the 95%-likely SE performance perspective, the CF-mMIMO system relying on OPA provides nearly identical performance for the cases of $C = 1$, $C = 2$, and $C = 4$, which is three times higher than that of the $C = M$ case. This result highlights the efficiency of OPA in maintaining consistent SE performance across varying numbers of CB clusters.

Figure 4 illustrates the convergence behaviour of the pro-

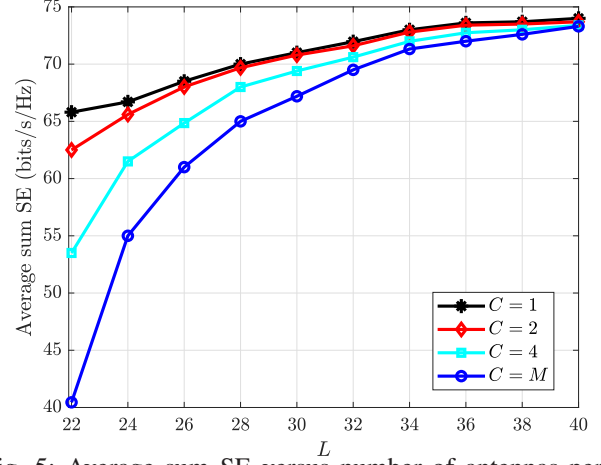


Fig. 5: Average sum SE versus number of antennas per AP, L , where $M = 10$, $K = 15$, $\text{FH}_{\max} = 14$ Gbps, $N = 2$, and $\bar{N} = 1$.

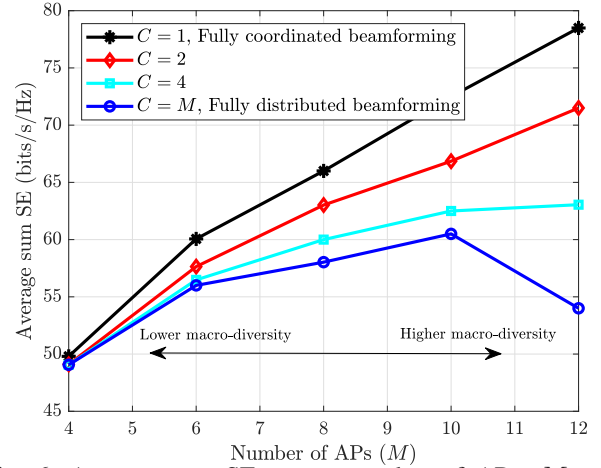


Fig. 6: Average sum SE versus number of APs, M , where $ML = 240$, $K = 15$, $\text{FH}_{\max} = 14$ Gbps, and $N = \bar{N} = 1$.

posed approach for different numbers of CB clusters. The algorithm is computationally efficient, with the number of iterations being minimal when $C = 1$ and maximal when $C = M$. This is because, for $C = 1$, there are K power allocation variables, while for C CB clusters, there are CK transmit power variables.

2) *Effect of the Number of Antennas Per AP*: Figure 5 shows the average sum-SE performance achieved by CF-mMIMO system for different number of transmit antennas at the AP. Increasing L has two effects on the sum-SE performance, namely, (i) increasing the diversity and array gain, and (ii) decreasing K_{\max} based on fronthaul constraint (50). The former effect becomes dominant under distributed scheme with $C = M$, which leads to a significant improvement in the SE performance. However, the latter effect becomes dominant under centralized CB scheme with $C = 1$. As a result, the performance gap between centralized and distributed scheme decreases with increasing L . Later, we will investigate the performance of the CF-mMIMO system under different fronthaul constraint values, as shown in Fig. 7. Simulation results in Fig. 5 also indicate that: 1) for high number of transmit

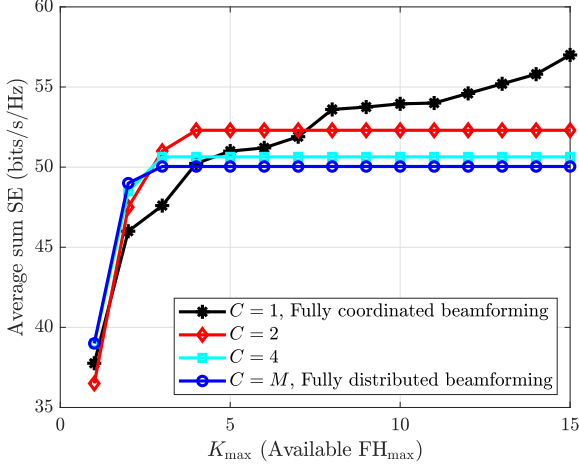


Fig. 7: Impact of the FH_{\max} on the sum SE, where $M = 10$, $K = 15$, $N = 2$, $\bar{N} = 1$, and $L = 12$.

antennas, CF-mMIMO with distributed beamforming relying on the proposed optimization solution has only negligible performance penalty, despite avoiding the high computational complexity for centralized CB and heavy overhead used for acquisition of CSI among large CB coordination sets. This result highlights the advantage of our optimization framework in reducing the need for beamforming coordination among a large number of APs; 2) a balance between performance, complexity, and scalability can be achieved by selecting an appropriate number of CB clusters, C , enabling partial cooperation to enhance performance while maintaining manageable complexity and fronthaul demands.

3) *Effect of the Number of APs*: Figures 6 depicts the average sum SE as a function of the number of APs for systems having the same total numbers of service antennas, i.e., $LM = 240$, but different number of APs. From this figure, we have the following observations

- Under fully coordinated beamforming and/or relatively large cooperation sizes, distributing antennas trivially achieves better performance thanks to added macro diversity on top of high-levels of interference cancellation due to CB design.
- On the other hand, for $C = M$ (fully distributed beamforming), a non-trivial trade-off between (per AP) beamforming capability and macro diversity should be achieved; i.e., further distributing antennas without beamforming coordination is detrimental.

4) *Effect of the Maximum Fronthaul Capacity*: In Fig. 7 we investigate the effect of the maximum available fronthaul capacity, FH_{\max} , on the performance of the CF-mMIMO system with the proposed optimization scheme under the fronthaul constraint. Different values of FH_{\max} , correspond to different values of K_{\max} , which are calculated based on (50). Upon increasing FH_{\max} the upper bound on the maximum number of users that each AP can serve, i.e., K_{\max} , increases. We note that in this figure, for each value of K_{\max} , we change the number of assigned users to the APs, K_m , from 1 to K_{\max} , and then choose the value that results in the maximum sum SE as

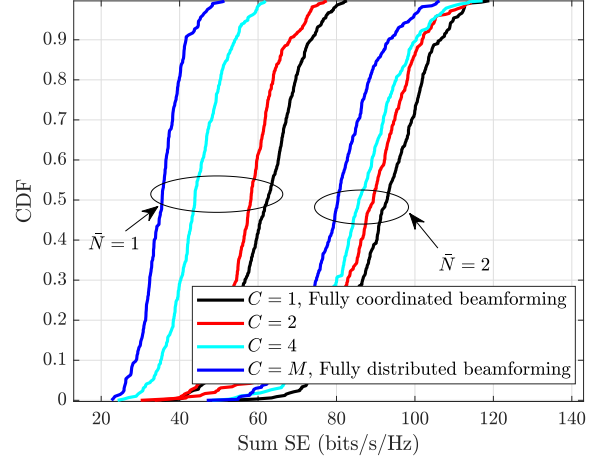


Fig. 8: CDF of the sum SE, where $M = 10$, $K = 15$, $N = 2$, $L = 18$, and $FH_{\max} = 18$ Gbps.

$$K_m^* = \arg \max_{K_m \in [1, \dots, K_{\max}]} \sum_{k \in \mathcal{K}} R_k(K_m). \quad (54)$$

From this figure, we have the following observations.

- The performance of CF-mMIMO with centralized CB notably increases with increasing K_{\max} . The main reason for this is the CB designs' capability to mitigate multi-user interference among users within the same CB cluster, which allows APs to select higher number of users to serve.
- For the considered CF-mMIMO system with distributed beamforming design $K_{\max} = 3$ is enough and increasing K_{\max} from 3 to 15 will not increase the sum-SE performance. This is due to the fact that distributed beamforming design exploits all degrees of freedom to mitigate its own interference to its assigned users, but not interference from other APs which is high for larger values of K_{\max} .
- In regimes with higher values of K_{\max} , which result from higher available FH_{\max} , centralized CB design outperforms other cases, while increasing the number of CB clusters leads to a reduction in the sum-SE performance. We also note that for the system with highly limited FH_{\max} , distributed beamforming design having the ability to provide a better performance/implementation complexity trade-off is undoubtedly a better choice.
- The relative performance gap between different cases changes when $K_{\max} < 8$. This change occurs because the CF-mMIMO system experiences varying levels of trade-offs between degrees of freedom for power optimization and inter-user interference cancellation for different numbers of CB clusters.
- Finally, our results indicate that under practical fronthaul limitations FH_{\max} , the proposed power allocation combined with simple distributed CB architecture can even outperform a computationally-heavy fully centralized CB when $K_{\max} \leq 4$.

5) *Effect of the Number of Downlink Data Streams*: In Fig. 8, we investigate the effect of number of downlink data stream \bar{N} on the sum-SE performance of the CF-mMIMO

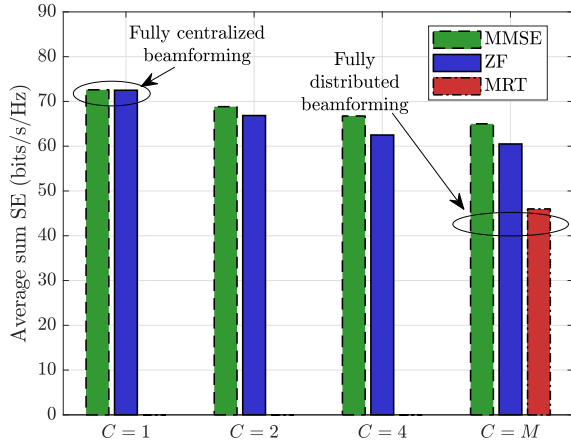


Fig. 9: Comparison between the sum SE achieved by different beamforming schemes, where $M = 10$, $K = 15$, $N = \bar{N} = 1$, $L = 24$, and $FH_{\max} = 14$ Gbps.

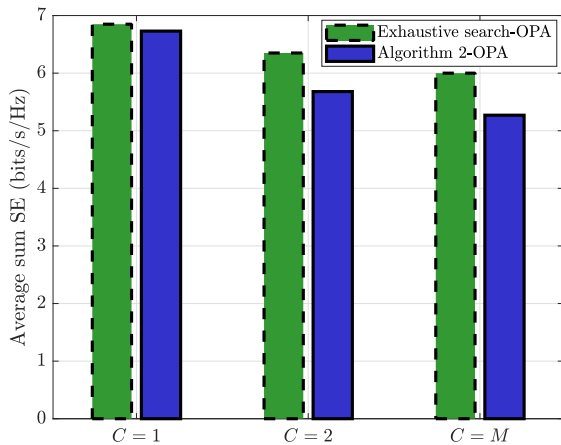


Fig. 10: Comparison between the heuristic user association Algorithm 2 and exhaustive search, where $M = 4$, $K = 3$, $N = 2$, $\bar{N} = 1$, $L = 8$, and $FH_{\max} = 3$ Gbps.

system for different number of CB clusters. We can see that using multiple data streams at the users greatly improves the sum SE for all cases. This is an interesting observation, as increasing \bar{N} has two impacts on the CF-mMIMO system: 1) enhancing the multiplexing gain and 2) increasing the amount of data traffic to be fronthauled between BBHs and BBLs, consequently reducing K_{\max} based on the fronthaul constraint (50). The increase in multiplexing gain dominates the sum-SE performance.

5) *Effect of the Beamforming Scheme*: In Fig. 9, we compare the performance of a CF-mMIMO system using ZF-based beamforming design and the MMSE scheme for different numbers of CB clusters. Moreover, we present results for the fully distributed MRT scheme. Simulation results indicate that the performance gap between ZF and MMSE is minimal, particularly for a smaller number of CB clusters. In the fully distributed case, MMSE and ZF beamforming schemes achieve sum-SE performance gains of 39% and 30% over the MRT scheme, respectively.

Finally, in Fig. 10, we benchmark the proposed heuristic user association algorithm (Algorithm 2) against an optimal approach using exhaustive search. A small system setup comprising 4 APs and 3 users is considered to enable the implementation of exhaustive search. The results demonstrate that the proposed heuristic approach achieves near-optimal performance in the fully centralized case with $C = 1$, while significantly reducing computational complexity. As the number of CB clusters increases, the performance loss of the heuristic user association algorithm grows; for the fully distributed case, which corresponds to the highest number of CB clusters, the performance loss remains below 14%.

VI. CONCLUSIONS

In this paper, we have provided a comprehensive analytical framework for the fronthaul limited CF-mMIMO systems with multiple-antenna users and multiple-antenna APs relying on both CB and UC clustering. The proposed CF-mMIMO framework is very general and can cover different CF-mMIMO scenarios with different performance-overhead and complexity trade-offs. We proposed a large-scale fading-based optimization approach to maximize the sum SE under a total transmit power constraint and fronthaul constraint. Our optimized approach demonstrated significant sum-SE gains compared to the baseline, particularly for fully distributed CB designs. Specifically, it achieved sum-SE performance gains of up to 59%, 173%, 252%, and 312%, over EPA for the cases of $C = 1$, $C = 2$, $C = 4$, and $C = M$, respectively. Insights from the simulation results demonstrated that the number of APs, the number of antennas, and the maximum fronthaul capacity are the key factors determining the extent to which decentralizing the beamforming design, such as by reducing the number of CB clusters, enhances the system performance. For example, if either the number of transmit/receive antennas is large or the available fronthaul is small, distributed beamforming design offers a better performance/implementation complexity trade-off. Nevertheless, the sum-SE performance improvement of the centralized CB design is more pronounced for higher values of available FH_{\max} . Future work will explore user mobility, Doppler effects, and hardware impairments in fronthaul-limited user-centric CF-mMIMO systems with CB. Moreover, more realistic channel models will be investigated to enhance practical applicability and refine performance predictions.

APPENDIX A COMPUTATIONAL COMPLEXITY ANALYSIS

The complexity is counted as the number of real flops where a real addition, multiplication, or division is counted as one flop. Also, a complex addition and multiplication have two flops and six flops, respectively.

1) *Computational Complexity of Different Beamforming Designs*: The computational complexity of the proposed beamforming schemes is elaborated as follows. Beamforming matrix calculation of a given AP m in (15) for the CB cluster C_m can be divided into two parts, i.e., the calculation of SVD

of channel matrix $\hat{\mathbf{G}}_m$ as $\hat{\mathbf{G}}_m = \mathbf{U}_m \Sigma_m \mathbf{V}_m^H$ and that of $\mathbf{U}_m \Sigma_m^{-1} \mathbf{V}_m^H$.

- The flop count for SVD of complex-valued $(LC_m) \times (NU_m)$ channel matrix $\hat{\mathbf{G}}_m$ in (14) is $24NL^2U_mC_m^2 + 48N^2LU_m^2C_m + 54N^3U_m^3$ by treating every operation as complex multiplication [33].
- For the second part, calculating Σ_m^{-1} needs NU_m real divisions and calculating $\mathbf{U}_m \Sigma_m^{-1}$ with given Σ_m^{-1} needs $2LNC_mU_m$ real multiplications. Then multiplying $\mathbf{U}_m \Sigma_m^{-1}$ with \mathbf{V}_m^H needs $8LN^2C_mU_m^2 - 2LNC_mU_m$ flops.

Hence, the total flop count for the beamforming calculation is $\varpi = NU_m + 24NL^2U_mC_m^2 + 56N^2LU_m^2C_m + 54N^3U_m^3$.

2) *Complexity of Power Allocation:* In each iteration of Algorithm 2, the computational complexity of solving problem (35) is $\mathcal{O}(\sqrt{n_{l1} + n_{q1}}(n_{v1} + n_{l1} + n_{q1})n_{v1}^2)$, where $n_{v1} = KC(C+1)$ is the number of real-valued scalar decision variables with C is the number of CB clusters, $n_{l1} = M + K$ denotes the number of linear constraints, and $n_{q1} = KC^2$ is the number of quadratic constraints [34]. Therefore, the number of flops required by the Algorithm 1 is $\mathcal{O}(\sqrt{M + K + KC^2}(KC(2C+1) + M + K)(KC(C+1))^2)$.

REFERENCES

- [1] H. Q. Ngo, A. Ashikhmin, H. Yang, E. G. Larsson, and T. L. Marzetta, "Cell-free massive MIMO versus small cells," *IEEE Trans. Wireless Commun.*, vol. 16, no. 3, pp. 1834–1850, Mar. 2017.
- [2] H. Q. Ngo, G. Interdonato, E. G. Larsson, G. Caire, and J. G. Andrews, "Ultradense cell-free massive MIMO for 6G: Technical overview and open questions," *Proc. IEEE*, pp. 1–27, 2024.
- [3] M. Mohammadi, Z. Mobini, H. Q. Ngo, and M. Matthaiou, "Next-generation multiple access with cell-free massive MIMO," *Proc. IEEE*, vol. 112, no. 9, pp. 1372–1420, Sept. 2024.
- [4] S. Buzzi, C. D'Andrea, A. Zappone, and C. D'Elia, "User-centric 5G cellular networks: Resource allocation and comparison with the cell-free massive MIMO approach," *IEEE Trans. Wireless Commun.*, vol. 19, no. 2, pp. 1250–1264, Feb. 2020.
- [5] J. Denis and M. Assaad, "Improving cell-free massive MIMO networks performance: A user scheduling approach," *IEEE Trans. Wireless Commun.*, vol. 20, no. 11, pp. 7360–7374, Dec. 2021.
- [6] H. A. Ammar, R. Adve, S. Shahbazpanahi, G. Boudreau, and K. V. Srinivas, "Downlink resource allocation in multiuser cell-free MIMO networks with user-centric clustering," *IEEE Trans. Wireless Commun.*, vol. 21, no. 3, pp. 1482–1497, Mar. 2022.
- [7] H. Q. Ngo, L.-N. Tran, T. Q. Duong, M. Matthaiou, and E. G. Larsson, "On the total energy efficiency of cell-free massive MIMO," *IEEE Trans. Green Commun. and Networking*, vol. 2, no. 1, pp. 25–39, Mar. 2018.
- [8] G. Dong, H. Zhang, S. Jin, and D. Yuan, "Energy-efficiency-oriented joint user association and power allocation in distributed massive MIMO systems," *IEEE Trans. Veh. Technol.*, vol. 68, no. 6, pp. 5794–5808, June 2019.
- [9] R. Jiang, Q. Wang, H. Haas, and Z. Wang, "Joint user association and power allocation for cell-free visible light communication networks," *IEEE J. Sel. Areas Commun.*, vol. 36, no. 1, pp. 136–148, Jan. 2018.
- [10] C. Hao, T. T. Vu, H. Q. Ngo, M. N. Dao, X. Dang, C. Wang, and M. Matthaiou, "Joint user association and power control for cell-free massive MIMO," *IEEE Internet Things J.*, vol. 11, no. 9, pp. 15 823–15 841, May 2024.
- [11] H. Sun, X. Chen, Q. Shi, M. Hong, X. Fu, and N. D. Sidiropoulos, "Learning to optimize: Training deep neural networks for interference management," *IEEE Trans. Signal Process.*, vol. 66, no. 20, pp. 5438–5453, Oct. 2018.
- [12] W. Xu, Z. Yang, D. W. K. Ng, M. Levorato, Y. C. Eldar, and M. Debbah, "Edge learning for B5G networks with distributed signal processing: Semantic communication, edge computing, and wireless sensing," *IEEE J. Sel. Top. Signal Process.*, vol. 17, no. 1, pp. 9–39, Jan. 2023.
- [13] A.-A. Lee, Y.-S. Wang, and Y.-W. P. Hong, "Deep CSI compression and coordinated precoding for multicell downlink systems," in *Proc. IEEE Global Commun. Conf. (GLOBECOM)*, 2020, pp. 1–6.
- [14] G. Interdonato, M. Karlsson, E. Björnson, and E. G. Larsson, "Local partial zero-forcing precoding for cell-free massive MIMO," *IEEE Trans. Wireless Commun.*, vol. 19, no. 7, pp. 4758–4774, July 2020.
- [15] L. Du, L. Li, H. Q. Ngo, T. C. Mai, and M. Matthaiou, "Cell-free massive MIMO: Joint maximum-ratio and zero-forcing precoder with power control," *IEEE Trans. Commun.*, vol. 69, no. 6, pp. 3741–3756, June 2021.
- [16] E. Nayeibi, A. Ashikhmin, T. L. Marzetta, H. Yang, and B. D. Rao, "Precoding and power optimization in cell-free massive MIMO systems," *IEEE Trans. Wireless Commun.*, vol. 16, no. 7, pp. 4445–4459, July 2017.
- [17] P. Liu, K. Luo, D. Chen, and T. Jiang, "Spectral efficiency analysis of cell-free massive MIMO systems with zero-forcing detector," *IEEE Trans. Wireless Commun.*, vol. 19, no. 2, pp. 795–807, Feb. 2020.
- [18] E. Björnson and L. Sanguinetti, "Making cell-free massive MIMO competitive with MMSE processing and centralized implementation," *IEEE Trans. Wireless Commun.*, vol. 19, no. 1, pp. 77–90, Jan. 2020.
- [19] M. Mohammadi, Z. Mobini, H. Q. Ngo, and M. Matthaiou, "Ten years of research advances in full-duplex massive MIMO," *IEEE Trans. Commun.*, vol. 73, no. 3, pp. 1756–1786, Mar. 2025.
- [20] T. C. Mai, H. Q. Ngo, and T. Q. Duong, "Downlink spectral efficiency of cell-free massive MIMO systems with multi-antenna users," *IEEE Trans. Commun.*, vol. 68, no. 8, pp. 4803–4815, Aug. 2020.
- [21] M. Bashar, H. Q. Ngo, K. Cumanan, A. G. Burr, P. Xiao, E. Björnson, and E. G. Larsson, "Uplink spectral and energy efficiency of cell-free massive MIMO with optimal uniform quantization," *IEEE Trans. Commun.*, vol. 69, no. 1, pp. 223–245, Jan. 2021.
- [22] M. Guenach, A. A. Gorji, and A. Bourdoux, "Joint power control and access point scheduling in fronthaul-constrained uplink cell-free massive MIMO systems," *IEEE Trans. Commun.*, vol. 69, no. 4, pp. 2709–2722, Apr. 2021.
- [23] X. Xia, P. Zhu, J. Li, H. Wu, D. Wang, Y. Xin, and X. You, "Joint user selection and transceiver design for cell-free with network-assisted full duplexing," *IEEE Trans. Wireless Commun.*, vol. 20, no. 12, pp. 7856–7870, Dec. 2021.
- [24] J. Yao, J. Xu, W. Xu, D. W. K. Ng, C. Yuen, and X. You, "Robust beamforming design for RIS-aided cell-free systems with CSI uncertainties and capacity-limited backhaul," *IEEE Trans. Wireless Commun.*, vol. 71, no. 8, pp. 4636–4649, Aug. 2023.
- [25] H. A. Ammar, R. Adve, S. Shahbazpanahi, G. Boudreau, and K. V. Srinivas, "Distributed resource allocation optimization for user-centric cell-free MIMO networks," *IEEE Trans. Wireless Commun.*, vol. 21, no. 5, pp. 3099–3115, May 2022.
- [26] T. Wang, C.-K. Wen, S. Jin, and G. Y. Li, "Deep learning-based CSI feedback approach for time-varying massive MIMO channels," *IEEE Wireless Commun. Lett.*, vol. 8, no. 2, pp. 416–419, Apr. 2019.
- [27] M. Urlea and S. Loyka, "Simple closed-form approximations for achievable information rates of coded modulation systems," *J. Lightw. Technol.*, vol. 39, no. 5, pp. 1306–1311, Mar. 2021.
- [28] D. R. Hunter and K. Lange, "A tutorial on MM algorithms," *The American Statistician*, no. 1, pp. 30–37, Feb. 2004.
- [29] T. T. Vu, D. T. Ngo, M. N. Dao, S. Durrani, and R. H. Middleton, "Spectral and energy efficiency maximization for content-centric C-RANs with edge caching," *IEEE Trans. Commun.*, vol. 66, no. 12, pp. 6628–6642, Dec. 2018.
- [30] M. Mohammadi, T. T. Vu, H. Q. Ngo, and M. Matthaiou, "Network-assisted full-duplex cell-free massive MIMO: Spectral and energy efficiencies," *IEEE J. Sel. Areas Commun.*, vol. 41, no. 9, pp. 2833–2851, Sept. 2023.
- [31] J. Rubio, A. Pascual-Iserte, D. P. Palomar, and A. Goldsmith, "Joint optimization of power and data transfer in multiuser MIMO systems," *IEEE Trans. Signal Process.*, vol. 65, no. 1, pp. 212–227, Jan. 2017.
- [32] T. T. Vu, D. T. Ngo, N. H. Tran, H. Q. Ngo, M. N. Dao, and R. H. Middleton, "Cell-free massive MIMO for wireless federated learning," *IEEE Trans. Wireless Commun.*, vol. 19, no. 10, pp. 6377–6392, June 2020.
- [33] Z. Shen, R. Chen, J. Andrews, R. Heath, and B. Evans, "Low complexity user selection algorithms for multiuser MIMO systems with block diagonalization," *IEEE Trans. Signal Process.*, vol. 54, no. 9, pp. 3658–3663, Sept. 2006.
- [34] H. H. M. Tam, H. D. Tuan, D. T. Ngo, T. Q. Duong, and H. V. Poor, "Joint load balancing and interference management for small-cell heterogeneous networks with limited backhaul capacity," *IEEE Trans. Wireless Commun.*, vol. 16, no. 2, pp. 872–884, Nov. 2017.